CHAPTER VI

GEOCHEMISTRY

Currently, geochemistry has become the most powerful tool available to unravel the origin and evolution of granitoid rocks; it can be used to classify granitoids, to establish genetic links between spatially associated granitoid rocks, reveal processes of their origin, to learn about the nature of source regions and potentially reveal information about their tectonic environments.

Hence, in the following pages geochemical data of granitoid rocks of Kumaun Higher Himalaya and also of the various nappes of Lesser Himalaya have been used to understand their petrogenetic behaviour.

ANALYTICAL TECHNIQUES

Representative samples of the granitoid rocks alongwith a few selected samples of associated schists, quartzites and amphibolites were broken into small pieces, coned and quartered. They were then crushed, powdered and milled (Â mesh). Pressed powder pellets were analysed by X-ray fluorescence method to determine major and trace elements, using Philips PV 9100 model XRF machine at Wadia Institute of Himalayan Geology (WIHG) Dehradun. Some samples were also analysed at National Geophysical Research Institute (NGRI), Hyderabad, by applying the same sample preparation technique using standard operating conditions on Philips Holland XRF model PW-1400.

The operating conditions were;

1. Major oxides : A_g anode, M_o filter, VAC path, 12 kv
2. Trace elements : A_g anode, A_g filter, Air path, 40 kv

Trace and Rare Earth Elements (REE) were also analysed at WIHG and NGRI using XRF and ICP-Mass spectrometer respectively. Acid dissolution procedure was adopted for preparing samples for ICP-Mass spectrometer. The ICP-MS used is the Plasma Quad PQ (Fissions Instruments, U.K.) controlled by an IBM PC-XT micro-computer and associated software.

Following standards were used for both XRF and ICP-MS at NGRI and WIHG:

CRPG (FRANCE) : GA, GH, GSN, MA-N

USGS (USA) : G2, GSP-1, RGN-1, QLO-1, AGV-1

GSJ (JAPAN) : JG2, JG1-a, JA2, JG3

IG GE (CHINA) : GSR1, GSR2,

In all 39 rock samples were analysed for major oxides out of which 28 samples were selected from the Central Crystallines, whereas 11 were those of the various crystalline nappes. Further 24 samples were analysed for trace element studies and 10 were selected for rare earth element studies. Samples from both the Central Crystallines as well as the crystalline nappes were similarly considered for trace and REE studies. The locations of the samples selected for geochemical analyses are shown (Figs. VI. A,B).

The geochemical diversity in granitoid rocks is ultimately a reflection of the composition(s) of the source region(s). Contrasting source regions are in turn, indicators of the geological environment (continental versus oceanic) and the tectonic setting (orogenic versus anorogenic). All these factors play their role in defining the spectrum of granitoid rocks and provide a sound basis for their classification (Bowden et al., 1984).

GEOLOGICAL SKETCH MAP OF HIGHER KUMAUN HIMALAYA SHOWING LOCATIONS OF SAMPLES SELECTED FOR CHEMICAL ANALYSES (For rock type details see Table VI. 1)

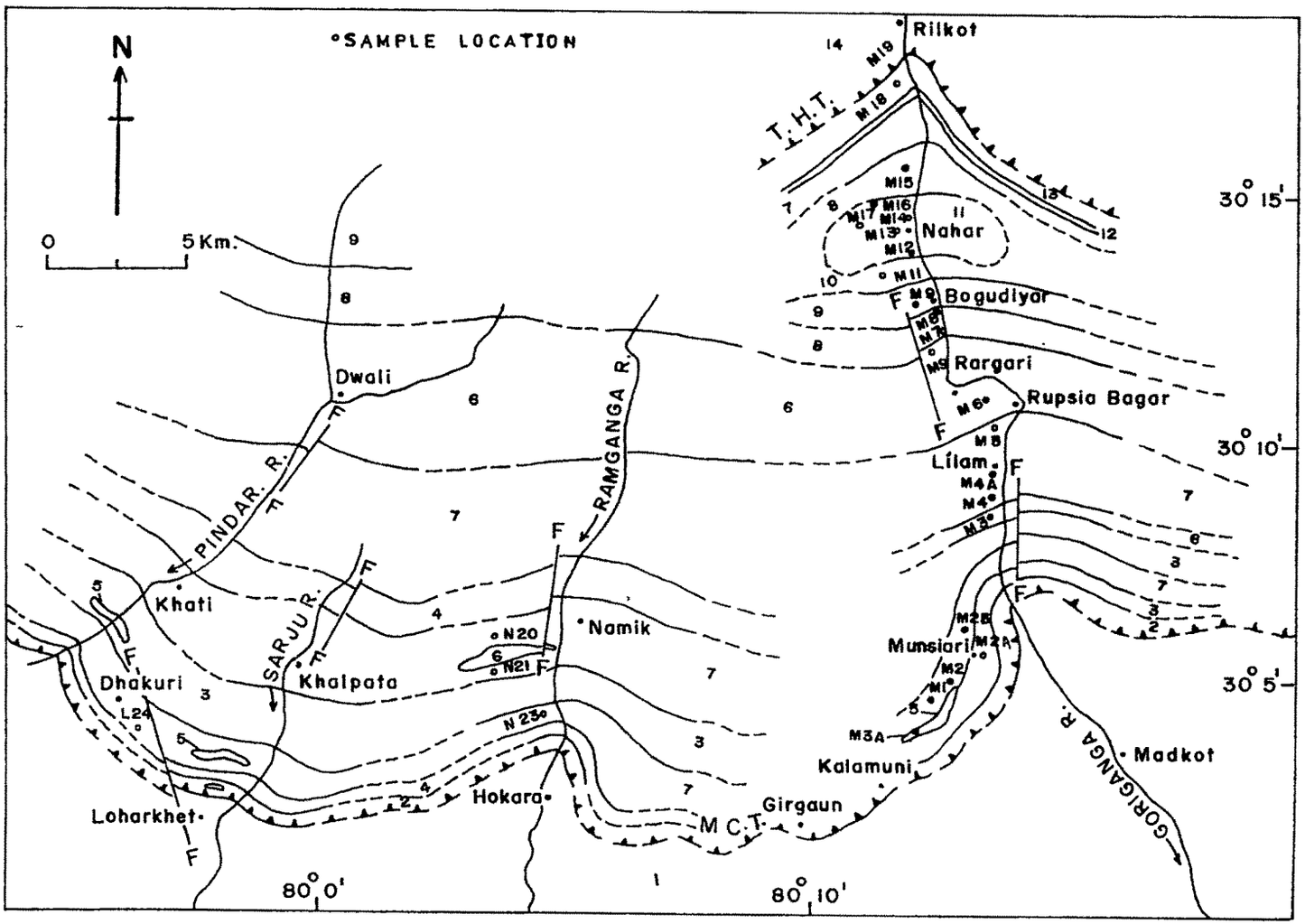

Fig. VI A

1. Metasedimentaries of Lesser Himalaya. 2. Phyllonites, Chlorite and Sericite schists. 3. Mica schists. 4. Garnet mica schists. 5. Amphibolites. 6. Micaceous quartzites. 7. Streaky, Augen and banded gneisses. 8. Garnetiferous augen gneisses and migmatites. 9. Garnetiferous kyanite gneisses. 10. Porphyroblastic and granitic gneisses. 11. Tourmaline and garnet bearing leucogranites with pegmatitic and aplitic veins. 12. Calcsilicate rocks. 13 Porphyroblastic mica schists. 14. Tethyan sediments. F—F Fault. ▲▲▲ Thrust. M.C.T Main Central Thrust. T.H.T Trans Himadri Thrust

GEOLOGICAL SKETCH MAP OF LESSER KUMAUN HIMALAYA CRYSTALLINE NAPPES SHOWING LOCATIONS OF SAMPLES SELECTED FOR CHEMICAL ANALYSES. (For rock type details see Table VI.1)

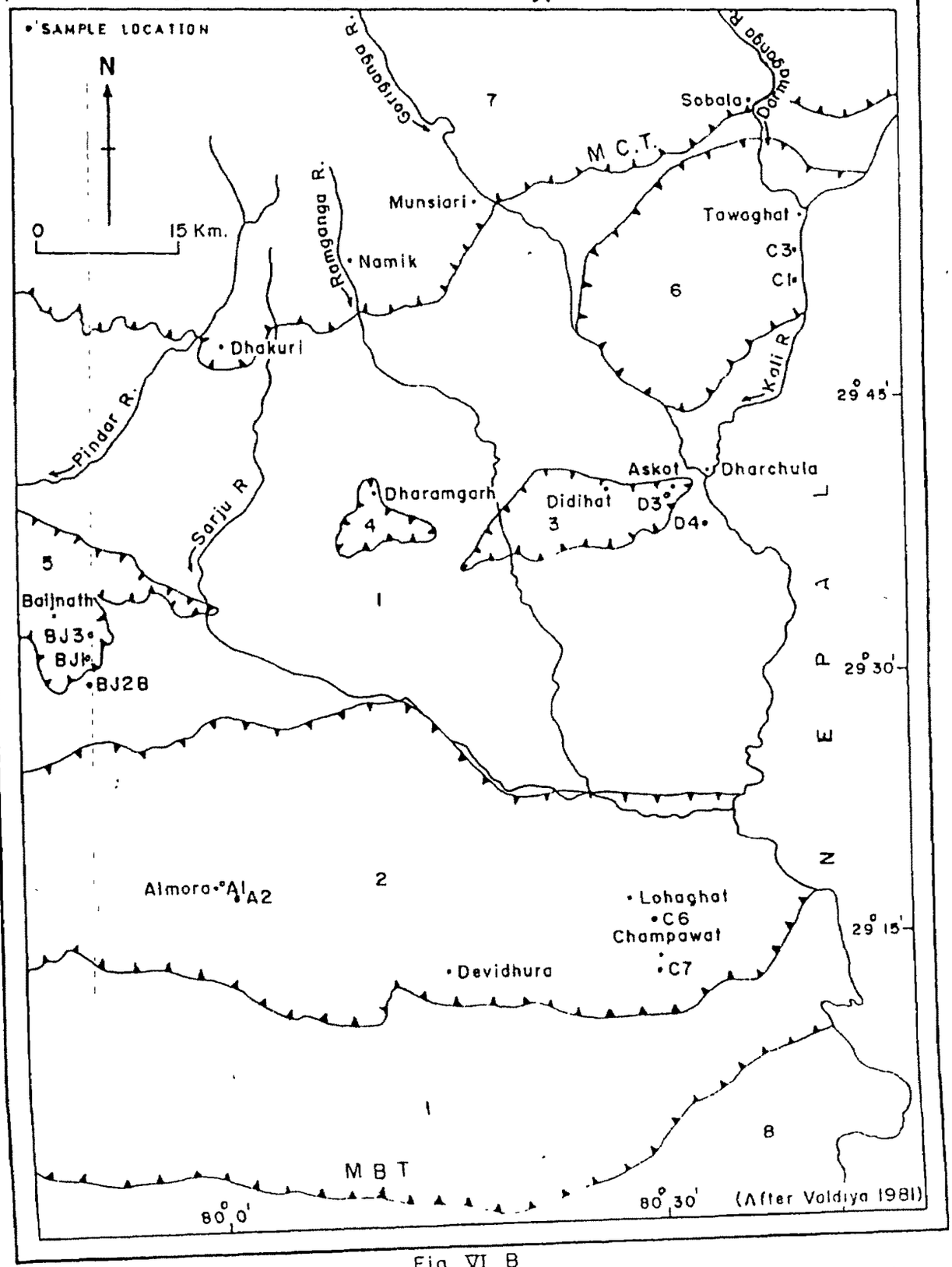

Fig VI B

1. Lesser Himalaya 2,3,4,5,&6 Almora, Askot, Dharamgarh, Baijnath and Chiplakot crystalline nappes 7 Higher Himalaya 8 Sub-Himalaya

MAJOR OXIDE CHEMISTRY

Major oxide data of rock samples of the study area, their Niggli Values and normative mineral compositions are given in Tables VI.1, VI.2 and VI.3. From Table VI.1, it is observed that SiO_2 varies from 63.97 to 75.05 weight percent for the granitoid rocks. The Al_2O_3 percentage is also quite high ranging from 11.60 - 17.90. The percentage of K_2O is found to be generally predominant over Na_2O. All the schistose samples show a preponderance of MgO over CaO which is a feature characteristic of argillaceous rocks. The granitoid rocks however are found depleted in Mgo, Cao and TiO_2. The Fe_2O_3(T) content varies from 1.11 to 6.21 percent for granitoid rocks but is higher in the associated schistose rocks where it ranges from 7.37 to even 16.75 percent.

The excess of alumina in the granitoid rocks appears as moderate normative corundum (2 - 3%), indicating a sedimentary origin. In the K_2O vs Na_2O diagram representing various fields of granites (Fig. VI.1) the granitoid samples are found scattered in the granite, adamellite, granodiorite as well as tonalite fields. However, in the Ab-Or-An (Fig. VI.2) ternary diagram (O'Connor, 1965) these rocks can be represented in the granite field. Similarly on the CaO - Na_2O - K_2O ternary diagram (Fig. VI.3) also almost all the granitoid samples fall in the granite field with only one or two falling in the adamellite and trondhjemite fields.

Table VI.1 MAJOR OXIDES ANALYSES OF ROCK SAMPLES

SL.NO.	SAMPLE NAME	ROCK TYPE	LOC.	SiO2	Al2O3	TiO2	CaO	MgO	Na2O	K2O	Fe2O3(T)	MnO	P2O5	TOTAL
22	M18	Sc	CCY	53.47	15.85	0.58	0.62	12.66	2.80	4.27	7.37	0.13	0.38	98.13
23	M19	Sc	CCY	53.32	9.30	0.59	3.16	22.61	0.00	2.77	8.14	0.12	0.07	100.08
27	M2A	Sc	CCY	44.43	11.01	1.68	0.14	11.98	0.46	9.01	16.75	0.13	0.17	95.76
AVG. SCHIST				50.41	12.05	0.95	1.31	15.75	1.09	5.35	10.75	0.13	0.21	97.99
37	M9	Qtz	CCY	81.21	9.68	0.19	1.05	0.00	4.06	2.24	1.22	0.04	0.04	99.73
34	M6	QtZ	CCY	73.83	14.21	0.01	0.71	0.06	3.75	5.47	1.66	0.01	0.07	99.78
29	M3	Qtz	CCY	69.97	15.71	0.00	0.81	0.12	3.89	5.15	1.80	0.02	0.15	97.62
AVG. QUARTZITE				75.00	13.20	0.07	0.86	0.06	3.90	4.29	1.56	0.02	0.09	99.04
10	D3	Gn	ASK	75.57	14.56	0.10	0.59	0.28	2.47	4.93	1.52	0.01	0.20	100.23
38	N21	Gn	CCY	75.05	13.38	0.12	1.27	0.23	4.09	2.16	1.45	0.03	0.05	97.83
5	BJ3	Gn	DHG	72.71	13.79	0.28	0.43	0.83	2.11	6.33	3.17	0.03	0.13	99.81
8	C6	Gn	CAM	72.45	16.73	0.17	0.50	1.32	7.28	1.28	0.65	0.01	0.13	100.52
39	N23	Gn	CCY	71.89	14.01	0.10	1.15	0.32	4.02	5.99	1.37	0.01	0.12	98.98
24	M1A	Gn	CCY	71.48	15.73	0.31	1.59	0.63	2.90	6.04	2.58	0.02	0.17	101.45
3	BJ1	Gn	BAJ	71.32	15.55	0.23	1.88	0.45	3.31	5.32	1.86	0.02	0.10	100.04
28	M2B	Gn	CCY	71.08	13.28	0.41	1.10	0.85	3.05	5.11	3.20	0.02	0.16	98.26
26	M20	Gn	CCY	70.62	15.19	0.38	0.77	1.32	3.94	4.27	2.88	0.03	0.17	99.57
12	L24	Gn	CCY	70.05	14.11	0.20	1.68	0.63	4.22	4.19	3.14	0.04	0.16	98.42
19	M15	Gn	CCY	69.38	13.04	0.72	1.22	1.75	3.60	2.94	4.79	0.11	0.12	97.67
35	M7	Gn	CCY	68.90	15.20	0.17	1.46	0.61	3.94	5.54	2.12	0.02	0.18	98.14
14	M10	Gn	CCY	68.67	14.35	0.66	1.38	1.51	4.02	2.84	4.90	0.10	0.18	98.61
33	M5	Gn	CCY	67.81	14.93	0.29	1.50	0.67	4.15	5.09	3.41	0.03	0.20	98.08
36	M8	Gn	CCY	66.98	14.10	0.65	1.02	1.27	3.99	3.16	5.63	0.11	0.17	97.08
32	M4A	Gn	CCY	66.09	15.42	0.54	3.34	1.15	2.92	4.57	4.70	0.05	0.15	98.93
7	C3	Gn	CHP	65.60	16.08	0.70	1.75	2.65	2.12	4.88	6.10	0.04	0.14	100.06
25	M2	Gn	CCY	65.12	16.39	0.57	2.58	1.64	4.11	2.69	4.80	0.07	0.27	98.24
6	C1	Gn	CHP	64.86	17.90	0.66	0.72	2.59	0.93	6.28	5.99	0.04	0.11	100.08
31	M4	Gn	CCY	64.63	15.71	0.56	2.69	1.51	4.24	4.79	4.47	0.05	0.29	98.94
13	M1	Gn	CCY	64.20	16.25	0.83	2.54	1.68	4.33	3.02	5.66	0.06	0.30	98.87
15	M11	Gn	CCY	63.97	16.29	0.68	1.18	2.17	4.05	3.58	6.21	0.18	0.28	98.59
AVG. GNEISSES				69.02	15.09	0.42	1.47	1.18	3.63	4.32	3.66	0.05	0.17	99.02
4	BJ2B	B	BAJ	52.48	11.38	0.94	10.62	8.78	3.24	0.30	11.35	0.15	0.13	99.37
30	M3A	B	CCY	50.90	10.38	1.71	12.62	6.94	2.04	0.62	13.83	0.17	0.16	99.37
11	D4	B	ASK	51.61	13.46	1.53	10.43	5.29	3.61	0.51	13.11	0.16	0.18	99.89
AVG. BASICS				51.66	11.74	1.39	11.22	7.00	2.96	0.48	12.76	0.16	0.16	99.54
16	M12	Gr	CCY	77.73	11.66	0.02	0.48	0.00	3.93	2.52	1.14	0.03	0.00	97.51
18	M14	Gr	CCY	72.78	13.92	0.11	0.70	0.17	3.91	5.16	1.74	0.02	0.08	98.59
21	M17	Gr	CCY	72.60	15.32	0.00	0.67	0.00	3.50	4.88	0.87	0.02	0.08	97.94
2	A2	Gr	ALM	72.24	15.33	0.32	1.01	0.54	3.07	4.89	2.75	0.05	0.18	100.38
17	M13	Gr	CCY	71.85	14.36	0.06	0.98	0.19	3.96	5.72	1.23	0.03	0.11	98.49
20	M16	Gr	CCY	70.20	15.65	0.03	1.29	0.16	3.82	6.49	1.11	0.00	0.15	98.90
9	C7	Gr	CAM	68.97	14.84	0.44	3.13	1.38	2.54	4.15	4.14	0.08	0.12	99.79
1	A1	Gr	ALM	68.84	17.48	0.14	1.22	0.02	4.19	4.72	1.62	0.02	0.22	98.47
AVG. GRANITE				71.90	14.82	0.14	1.19	0.31	3.62	4.82	1.83	0.03	0.12	98.76

CCY - Central Crystallines, ALM - Almora Nappe, BAJ - Baijnath Nappe, ASK - Askot Nappe, DHG - Dharamgarh Nappe, CHP - Chiplakot Nappe, CAM - Champawat Crystallines

Table VI.2 NIGGLI VALUES

SL. NO.	SAMPLE NAME	ROCK TYPE	LOC.	si	ti	p	k	mg	alk	c	fm	al
22	M18	Sc	CCY	135.08	1.11	0.41	0.50	0.79	13.87	1.69	60.57	23.86
23	M19	Sc	CCY	106.06	0.89	0.06	1.00	0.86	3.55	6.80	78.63	11.02
27	M2A	Sc	CCY	104.23	2.99	0.17	0.93	0.61	14.67	0.36	69.58	15.39
AVG. SCHIST				115.12	1.67	0.21	0.81	0.75	10.70	2.95	69.59	16.76
37	M9	Qtz	CCY	626.46	1.11	0.13	0.27	0.00	41.79	8.76	4.94	44.50
34	M6	QtZ	CCY	428.90	0.04	0.17	0.49	0.12	41.79	4.46	4.55	49.20
29	M3	Qtz	CCY	381.09	0.00	0.35	0.47	0.18	38.81	4.77	5.42	50.99
AVG. QUARTZITE				478.82	0.39	0.22	0.41	0.10	40.80	6.00	4.97	48.23
38	N21	Gn	CCY	473.74	0.58	0.13	0.26	0.32	34.06	8.67	6.93	50.34
10	D3	Gn	ASK	469.58	0.47	0.53	0.57	0.36	34.76	3.97	7.36	53.92
5	BJ3	Gn	DHG	407.72	1.19	0.31	0.66	0.42	34.44	2.61	16.86	46.08
39	N23	Gn	CCY	387.42	0.41	0.28	0.50	0.41	42.00	6.71	6.30	45.00
28	M2B	Gn	CCY	386.64	1.69	0.37	0.52	0.43	34.14	6.47	16.33	43.05
3	BJ1	Gn	BAJ	367.21	0.90	0.22	0.51	0.47	34.33	10.47	7.48	47.72
24	M1A	Gn	CCY	356.32	1.17	0.36	0.58	0.42	33.54	8.58	11.15	46.73
12	L24	Gn	CCY	354.08	0.77	0.35	0.40	0.35	34.52	9.19	13.78	42.51
26	M20	Gn	CCY	353.44	1.44	0.36	0.42	0.57	33.07	4.17	17.45	45.31
8	C6	Gn	CAM	348.34	0.62	0.27	0.10	0.85	38.23	2.60	11.23	47.94
19	M15	Gn	CCY	346.34	2.73	0.26	0.35	0.48	27.05	6.59	27.57	38.79
35	M7	Gn	CCY	344.84	0.65	0.39	0.48	0.48	37.16	7.91	9.59	45.34
33	M5	Gn	CCY	325.86	1.06	0.41	0.45	0.34	35.28	7.80	14.16	42.76
14	M10	Gn	CCY	325.83	2.38	0.37	0.32	0.43	27.35	7.09	24.98	40.58
36	M8	Gn	CCY	320.26	2.36	0.35	0.34	0.35	28.41	5.28	26.14	40.18
32	M4A	Gn	CCY	285.20	1.77	0.28	0.51	0.38	25.04	15.60	19.71	39.66
25	M2	Gn	CCY	274.67	1.83	0.49	0.30	0.46	24.28	11.77	22.75	41.20
6	C1	Gn	CHP	269.47	2.08	0.20	0.82	0.51	20.59	3.24	31.85	44.32
7	C3	Gn	CHP	267.55	2.17	0.24	0.60	0.51	21.28	7.72	31.91	39.09
31	M4	Gn	CCY	264.44	1.74	0.51	0.43	0.46	29.61	11.91	20.18	38.31
13	M1	Gn	CCY	260.80	2.56	0.52	0.31	0.42	25.12	11.16	24.37	39.34
15	M11	Gn	CCY	260.36	2.10	0.49	0.37	0.45	25.52	5.20	29.77	39.51
AVG. GNEISSES				338.64	1.48	0.35	0.44	0.45	30.90	7.49	18.08	43.53
11	D4	B	ASK	128.77	2.90	0.19	0.09	0.47	9.64	28.16	42.19	20.01
4	BJ2B	B	BAJ	122.96	1.67	0.13	0.06	0.63	7.88	26.92	49.30	15.89
30	M3A	B	CCY	120.84	3.08	0.16	0.17	0.53	5.69	32.42	47.21	14.69
AVG. BASICS				124.19	2.55	0.16	0.10	0.54	7.74	29.17	46.23	16.86
16	M12	Gr	CCY	574.28	0.11	0.00	0.30	0.00	40.42	3.84	4.40	51.34
21	M17	Gr	CCY	430.28	0.00	0.20	0.48	0.00	38.94	4.30	2.65	54.11
18	M14	Gr	CCY	423.36	0.49	0.20	0.46	0.26	41.60	4.41	5.74	48.26
17	M13	Gr	CCY	396.93	0.25	0.26	0.49	0.31	41.77	5.86	5.09	47.28
2	A2	Gr	ALM	387.53	1.30	0.41	0.51	0.36	33.02	5.86	12.11	49.01
20	M16	Gr	CCY	361.15	0.12	0.33	0.53	0.30	40.74	7.18	4.09	47.98
1	A1	Gr	ALM	348.12	0.54	0.48	0.43	0.03	36.12	6.68	4.53	52.68
9	C7	Gr	CAM	314.28	1.52	0.23	0.52	0.46	23.51	15.43	20.76	40.30
AVG. GRANITE				404.49	0.54	0.26	0.46	0.22	37.01	6.69	7.42	48.87

Table VI.3 CIPW Norms

SL. NO.	SAMPLE NAME	ROCK TYPE	LOC	ap	il	mt	hem	Or	Ab	An	C	Hy	Q
34	M6	Qtz	CCY	0.0976	0.0190	0.2407	0.0000	32.3545	31.6935	3.0724	0.9778	2.7356	28.5154
29	M3	Qtz	CCY	0.2092	0.0000	0.2610	0.0000	30.4617	32.8768	3.0520	2.6022	3.1215	24.8796
38	M21	Gn	CCY	0.0697	0.2280	0.2103	0.0000	12.7762	34.5671	5.9816	2.1128	2.6499	39.1592
10	D3	Gn	ASK	0.2789	0.1900	0.2204	0.0000	29.1604	20.8755	1.6368	4.5463	2.9176	40.2127
5	DJ3	Gn	DHG	0.1813	0.5320	0.4596	0.0000	37.4413	17.8329	1.2948	2.9749	6.5820	32.3633
28	M2B	Gn	CCY	0.2231	0.7790	0.4640	0.0000	30.2251	25.7774	4.4270	1.0951	6.4645	28.6417
3	BJ1	Gn	BAJ	0.1394	0.4370	0.2697	0.0000	31.4672	27.9748	8.6868	1.1445	3.6611	26.1487
24	M1A	Gn	CCY	0.2370	0.5890	0.3741	0.0000	35.7260	24.5097	6.7949	1.9119	5.1077	26.0256
12	L24	Gn	CCY	0.2231	0.3800	0.4553	0.0000	24.7834	35.6658	7.1430	0.1269	3.5177	24.5266
26	M20	Gn	CCY	0.2370	0.7220	0.4176	0.0000	25.2566	33.2994	2.7242	3.0751	7.1874	26.4665
8	C6	Gn	CAM	0.1813	0.3230	0.0942	0.0000	7.5711	61.5277	1.6423	2.7617	4.0384	22.2524
19	N15	Gn	CCY	0.1673	1.3680	0.6946	0.0000	17.3898	30.4258	5.2812	1.9895	10.6953	29.4397
35	M7	Gn	CCY	0.2510	0.3230	0.3074	0.0000	32.7685	33.2994	6.0850	0.4740	4.5676	19.8810
33	M5	Gn	CCY	0.2789	0.5510	0.4944	0.0000	30.1068	35.0742	6.1543	0.3213	6.5417	18.3459
14	M10	Gn	CCY	0.2510	1.2540	0.7105	0.0000	16.7983	33.9755	5.6878	2.5679	10.3668	26.7350
36	M8	Gn	CCY	0.2370	1.2350	0.8163	0.0000	18.6911	33.7219	3.9653	2.6520	10.9275	24.5696
32	M4A	Gn	CCY	0.2092	1.0260	0.6815	0.0000	27.0311	24.6787	15.4186	0.1500	6.5089	21.5275
25	M2	Gn	CCY	0.3765	1.0830	0.6960	0.0000	15.9111	34.7361	11.0635	2.6502	10.6835	20.7252
6	C1	Gn	CHP	0.1534	1.2540	0.8686	0.0000	37.1455	7.8600	2.8636	8.5040	14.7753	26.5150
7	C3	Gn	CHP	0.1952	1.3300	0.8845	0.0000	28.8627	17.9174	7.7830	4.4413	15.0318	23.4455
31	M4	Gn	CCY	0.4044	1.0640	0.6482	0.0000	28.3323	35.8348	9.6397	1.4302	7.2019	12.9750
13	M1	Gn	CCY	0.4183	1.5770	0.8207	0.0000	17.8630	36.5955	10.6711	1.9341	11.7026	16.9556
15	M11	Gn	CCY	0.3904	1.2920	0.9004	0.0000	21.1753	34.2290	4.0489	4.2568	14.0372	17.8259
16	M12	Gr	CCY	0.0000	0.0380	0.1653	0.0000	14.9055	33.2148	2.3829	1.5858	1.7540	43.4338
21	M17	Gr	CCY	0.1115	0.0000	0.1361	0.0000	28.8647	29.5806	2.8092	3.2359	1.3637	31.7556
18	M14	Gr	CCY	0.1115	0.2090	0.2523	0.0000	30.5209	33.0458	2.9582	0.8029	2.9710	27.6259
17	M13	Gr	CCY	0.1534	0.1140	0.1784	0.0000	33.8332	33.4684	4.1543	0.1141	2.3040	24.0405
2	A2	Gr	ALM	0.2510	0.6080	0.3987	0.0000	28.9328	25.9465	3.8510	3.5602	5.1326	31.4948
20	M16	Gr	CCY	0.2092	0.0570	0.1609	0.0000	38.3870	32.2852	5.4348	0.3291	2.0904	19.8097
1	A1	Gr	ALM	0.3068	0.2660	0.2349	0.0000	27.9183	35.4123	4.6351	3.7644	2.3584	23.3544
9	C7	Gr	CAM	0.1673	0.8360	0.6003	0.0000	24.5468	21.4671	14.7629	0.7415	9.2135	27.2658

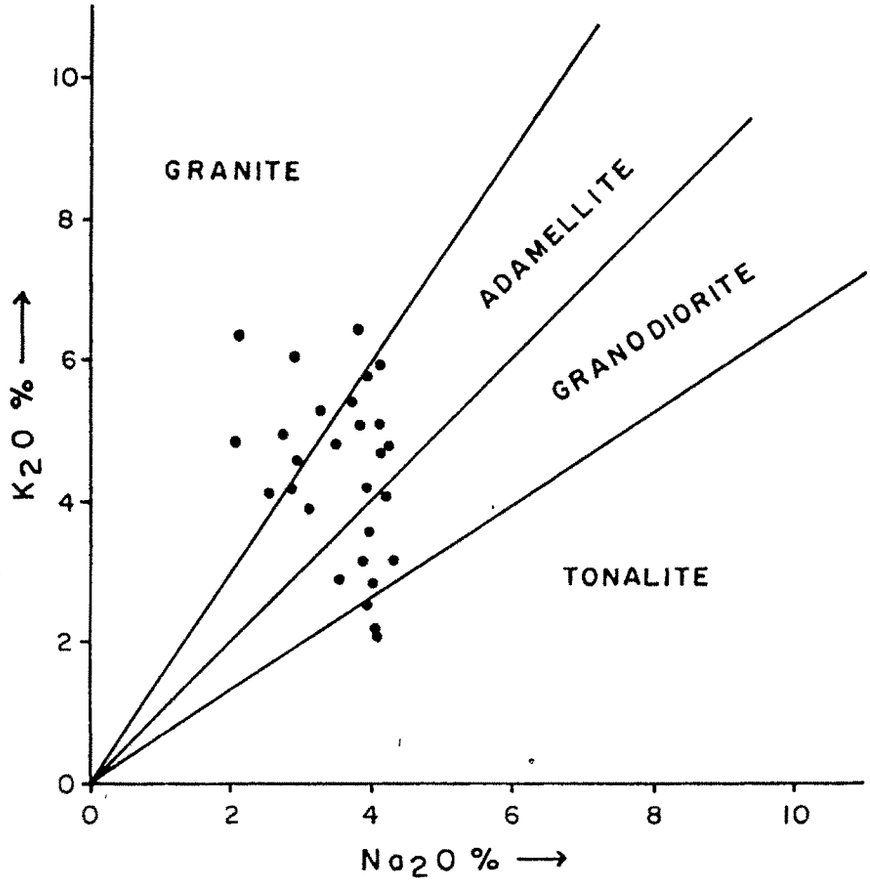

Fig. VI.1 K_2O vs Na_2O diagram

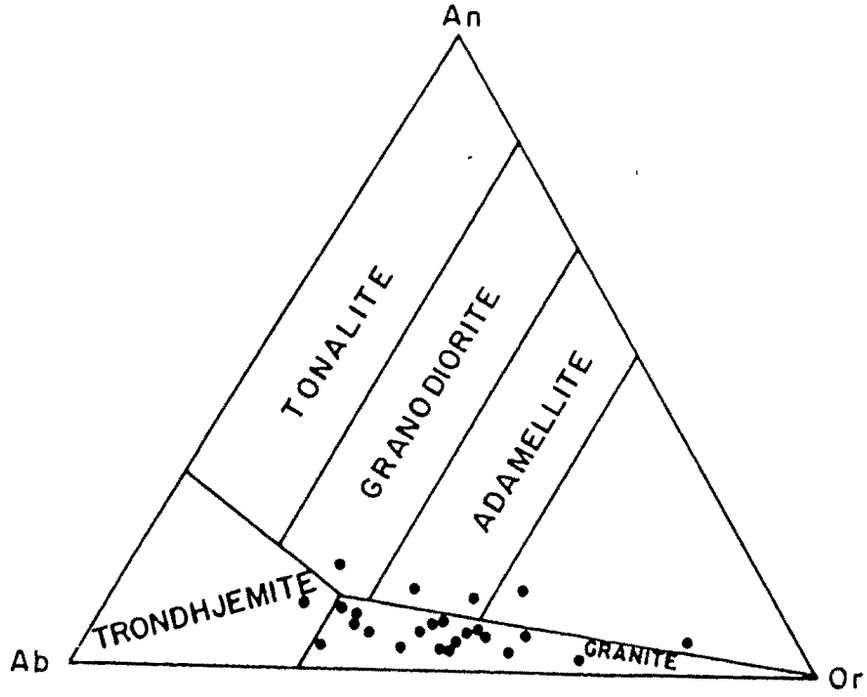

Fig. vi. 2 Ab – Or – An diagram (O'Connor, 1965)

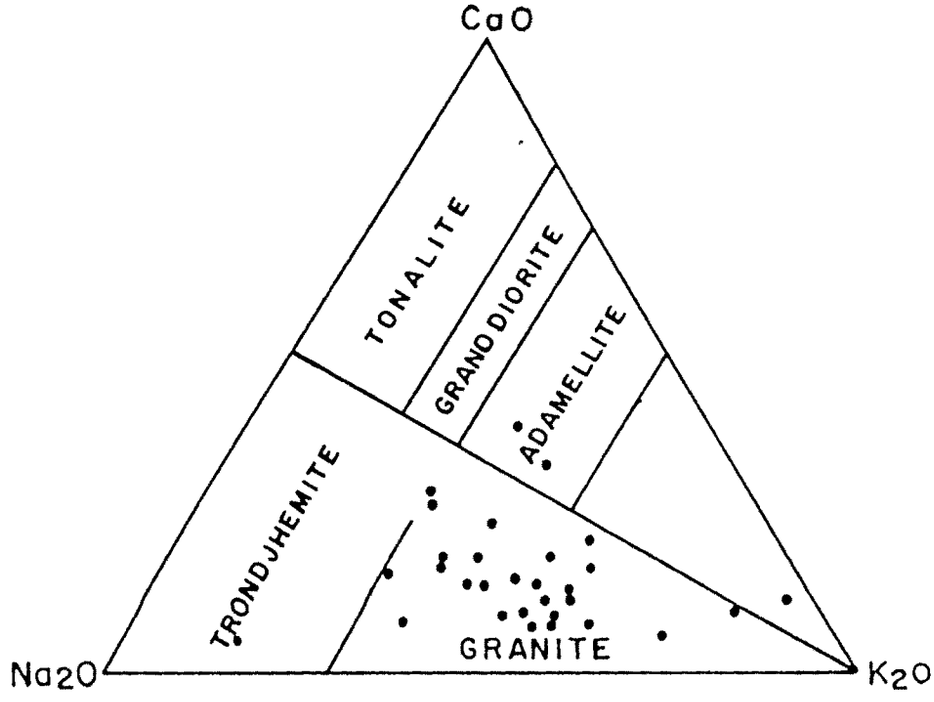

Fig. vi 3 Ternary variation diagram for deformed granite compositions (O'Connor, 1965)

The difference in the lithological and mineralogical characters of various rock samples is brought out by the bulk rock chemistry, i.e., when plots of their Niggli values were prepared (si against mg, fm+c, ti, p, al, k and alk). On binary diagrams (Fig. VI.4 a to g) they got better resolved, all forming a single cluster indicating a common source. The granitoids show a general depletion in mg, ti, p against increasing si Niggli values. Alk and al are found to show an increase with increasing si values fm+c is found to decrease with increasing si, whereas the schists show an increase in fm+c.

A careful examination of the Niggli values (Table VI.2) of granitoid rocks reveals that alk shows an increase with increasing si value, while ti, p, c, al, fm and mg show a systematic decrease with increasing si, a few samples exhibiting a certain amount of deviation which are to be expected in the sedimentary formations and have been observed by Shaw (1956). The Niggli values of the schists, amphibolites, quartzites as well as the granitoid rocks have also been represented in two triangular diagrams, viz., alk – al – fm+c and fm – c – al (Fig. VI.5 and 6) respectively. The amphibolites and schists exhibit higher values of fm+c and fm, whereas the granitoids and the quartzites are depleted in the same. The granitoids are all grouped together alongwith the quartzites in a single cluster with high values of al and alk as compared to the schists and amphibolites.

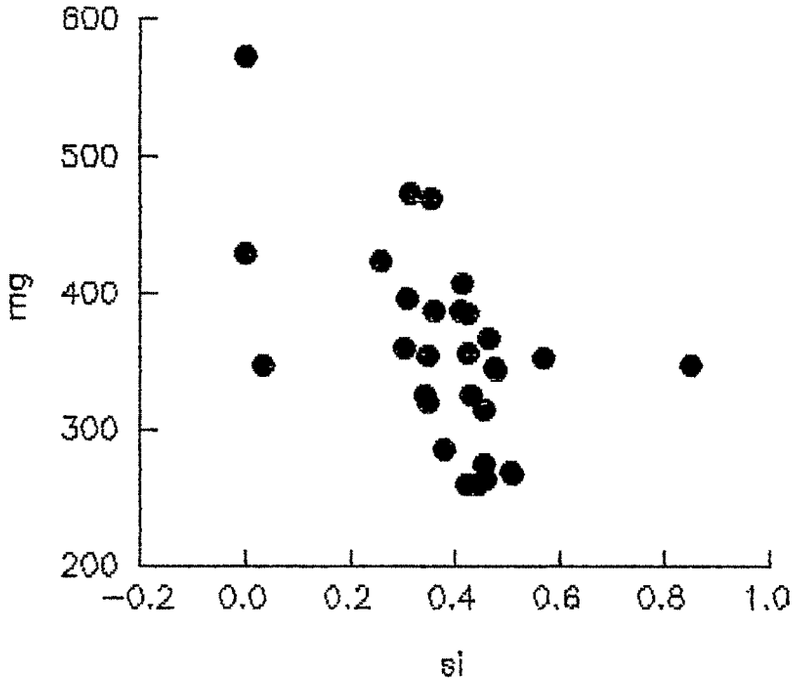

Fig. VI.4 a : mg vs si

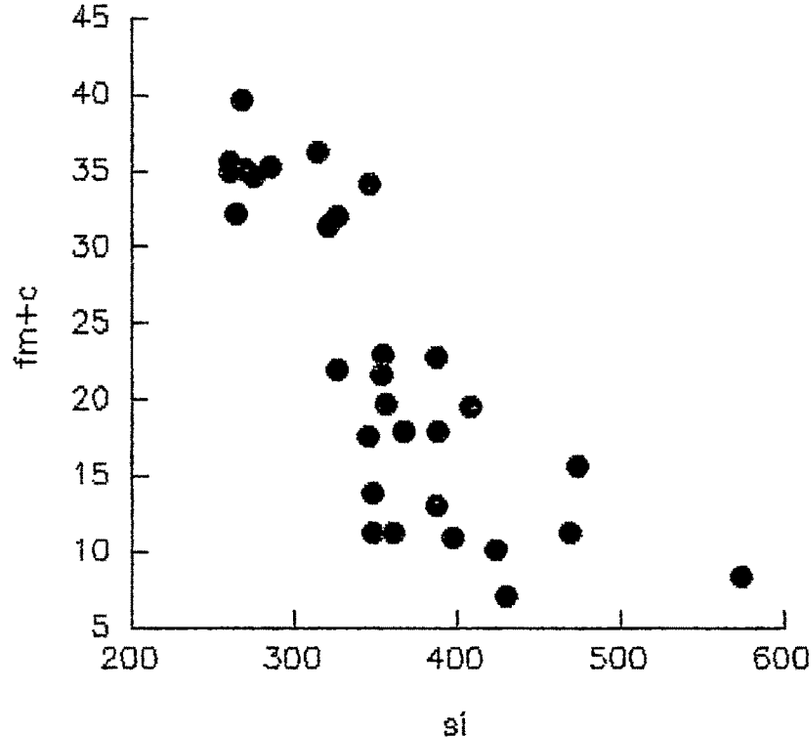

Fig. VI.4 b : fm+c vs si

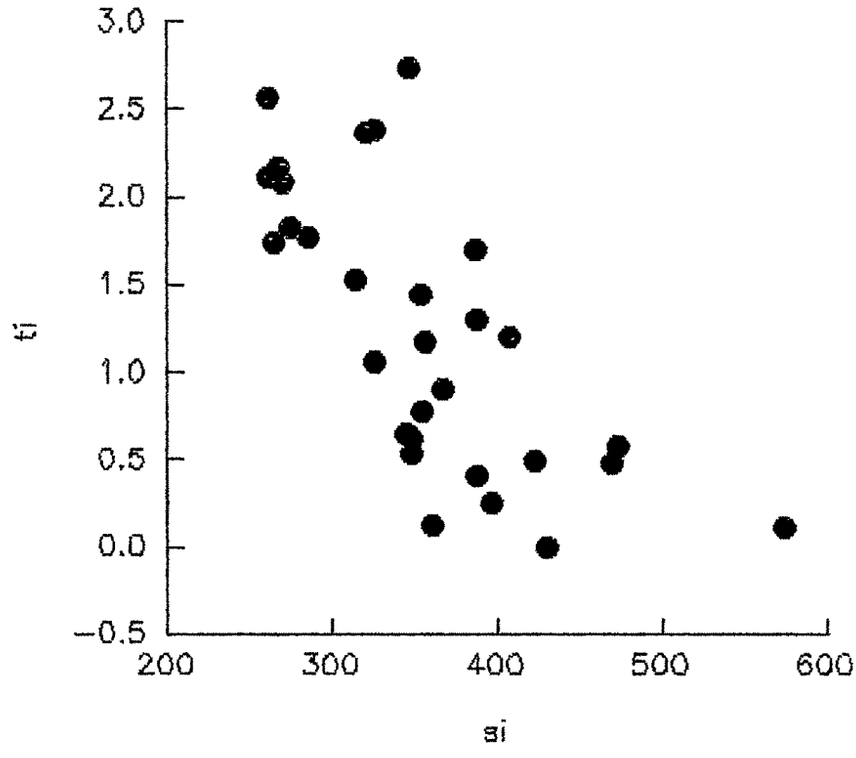

Fig. VI.4 c : ti vs si

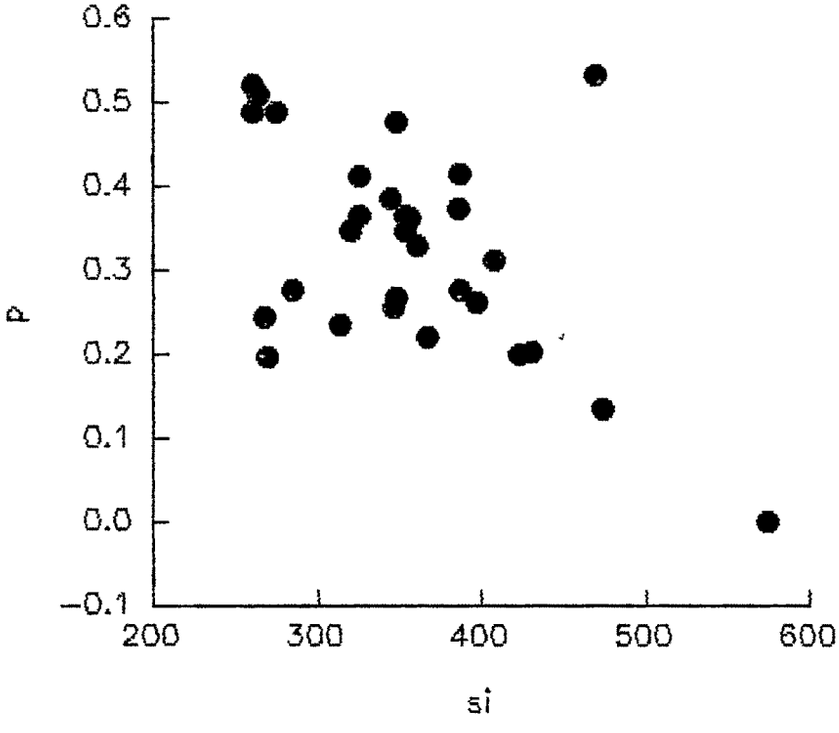

Fig. VI.4 d : p vs si

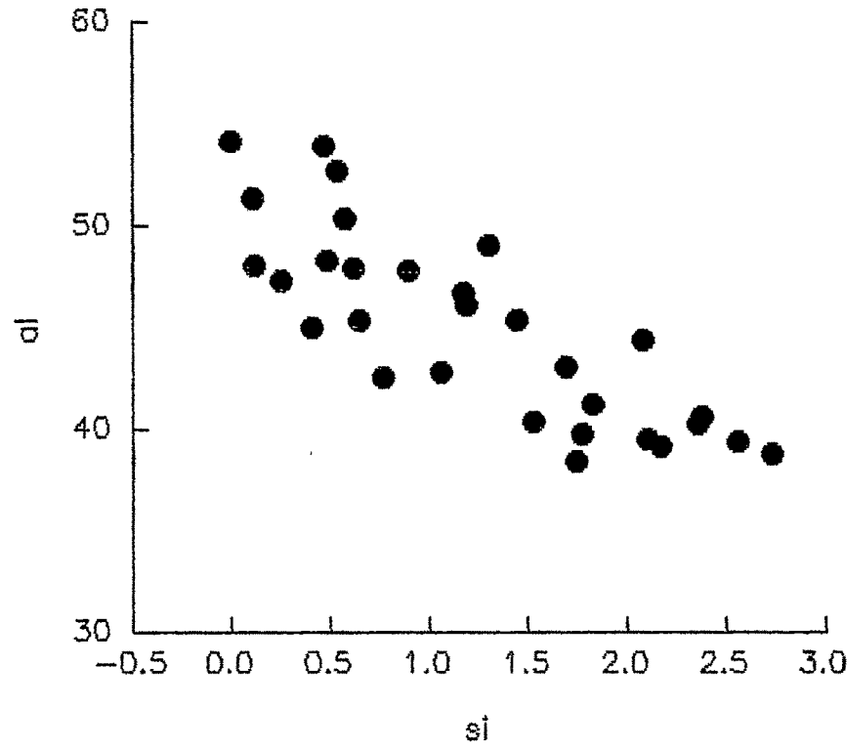

Fig. VI.4 e : al vs si

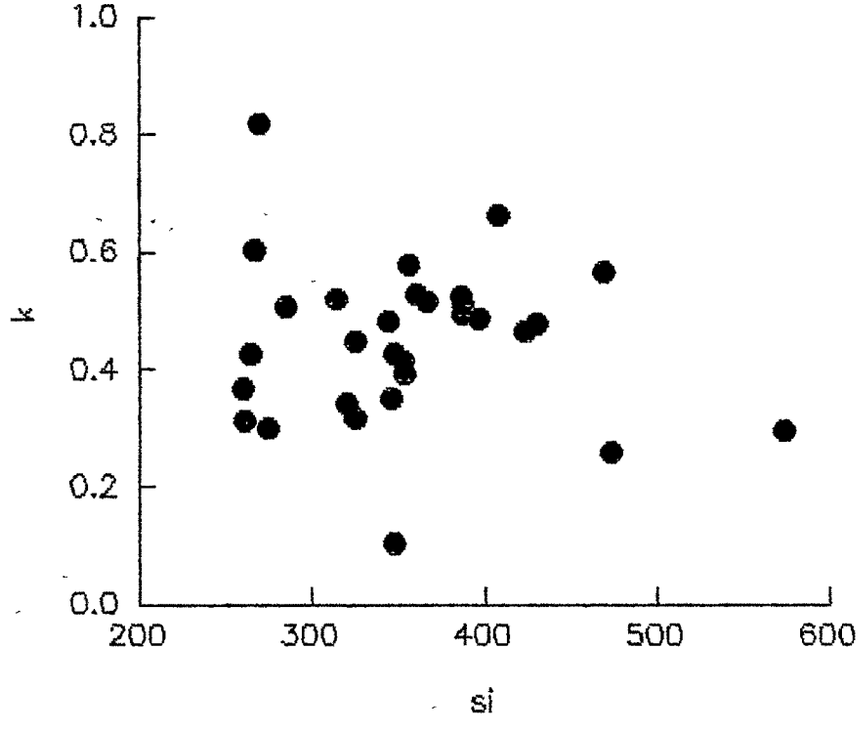

Fig. VI.4 f : k vs si

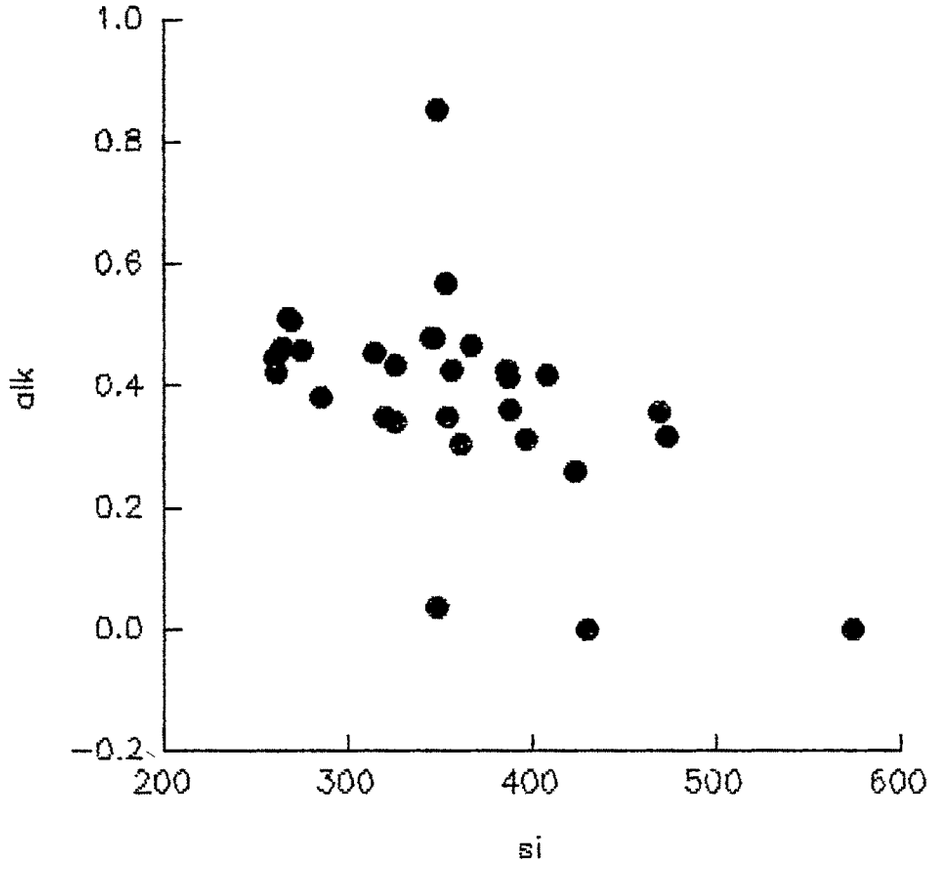

Fig. VI.4 g : alk vs si

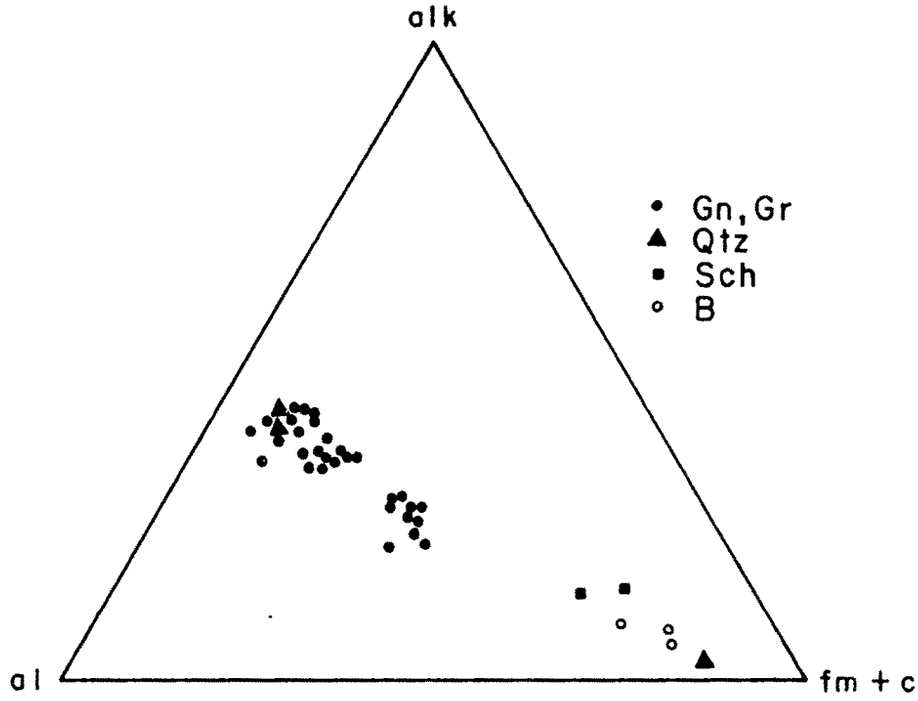

Fig. vi. 5 alk–al – fm + c diagram

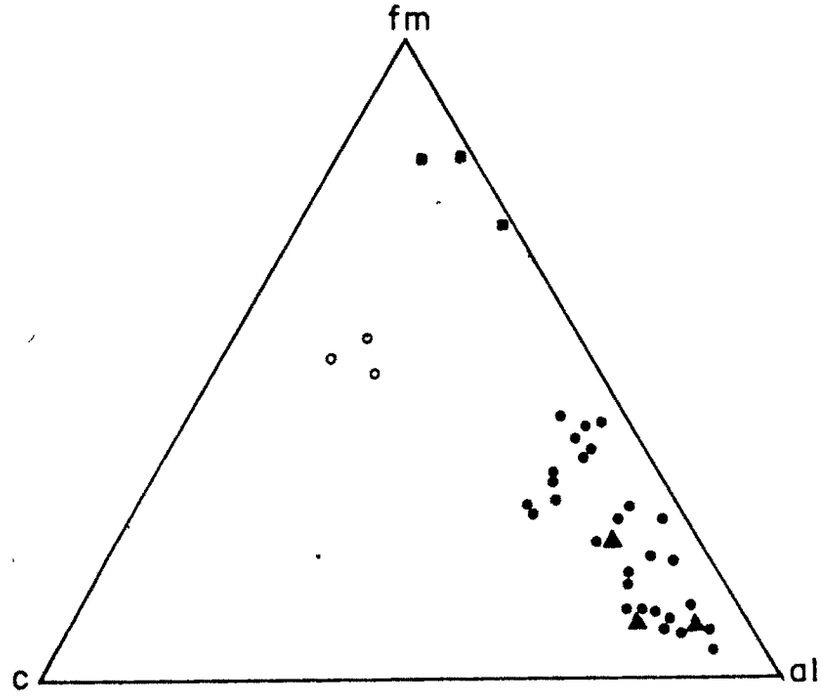

Fig. vi. 6 fm – c – al diagram

SiO_2 against Na_2O, K_2O, P_2O_5, CaO, Al_2O_3, TiO_2, MgO, MnO and Fe_2O_3(T) plots have been prepared to understand the behaviour of these elements with variations in silica content in the granitoid rocks of the study area (Fig. VI.7 a to i). Examination of these Harker variation diagrams indicate that the major oxides CaO, MgO, MnO, P_2O_5, TiO_2 and Fe_2O_3(T) define linear negative trends with increase in silica, that is all these major oxides decrease with increasing silica. The depletion of ferromagnesian minerals is accounted for by a general decrease of biotite as is also revealed by the petrographic details of the granitoid rocks. These rocks are more abundant in muscovite rather than biotite. Moreover, opaque minerals are also found in biotite. Major oxide K_2O shows linear positive trend with increase in silica, hence with increase in silica, K_2O tends to increase, while Na_2O does not show any appreciable change with increase in silica and Al_2O_3 decreases with increase in SiO_2. A progressive enrichment of K_2O over Na_2O can also be made out from the major oxide variation diagrams, however, CaO declines with increasing silica indicating higher K-feldspar content as compared to plagioclase feldspar.

The average major oxide data of the granitoid rocks of the study area are compiled alongwith average sediment, average paragneiss and average phyllites, schists and paragneiss for comparison in Table VI.4. A careful study of the various major oxides reveals that the granitoids of present study show an enrichment of SiO_2, Na_2O and K_2O and a depletion of Fe_2O_3(T), MgO, CaO

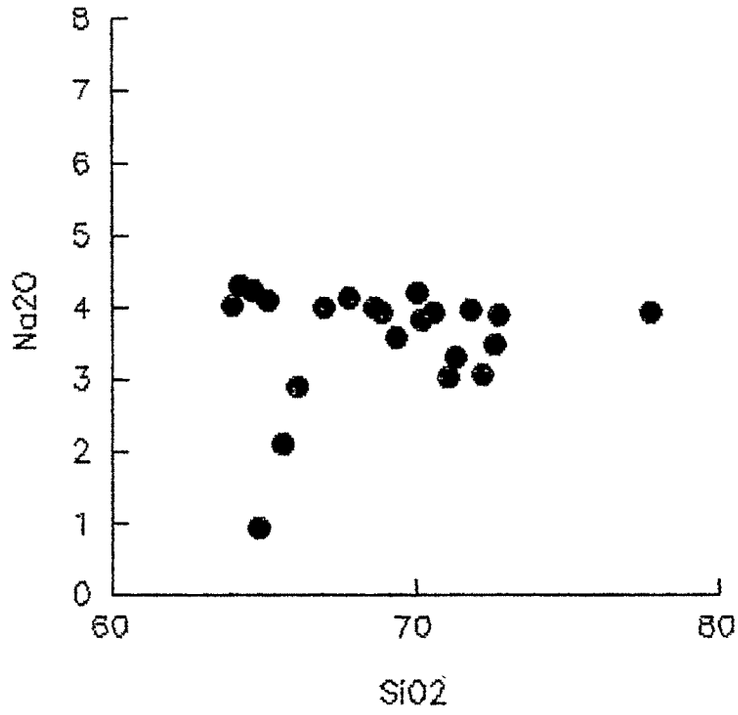

Fig. VI.7 a : Na2O vs SiO2

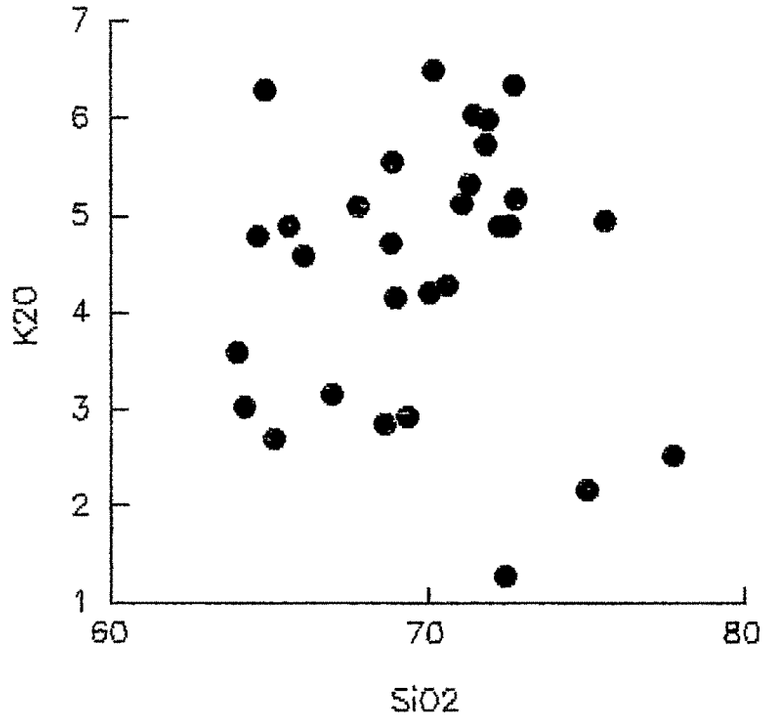

Fig. VI.7 b : K2O vs SiO2

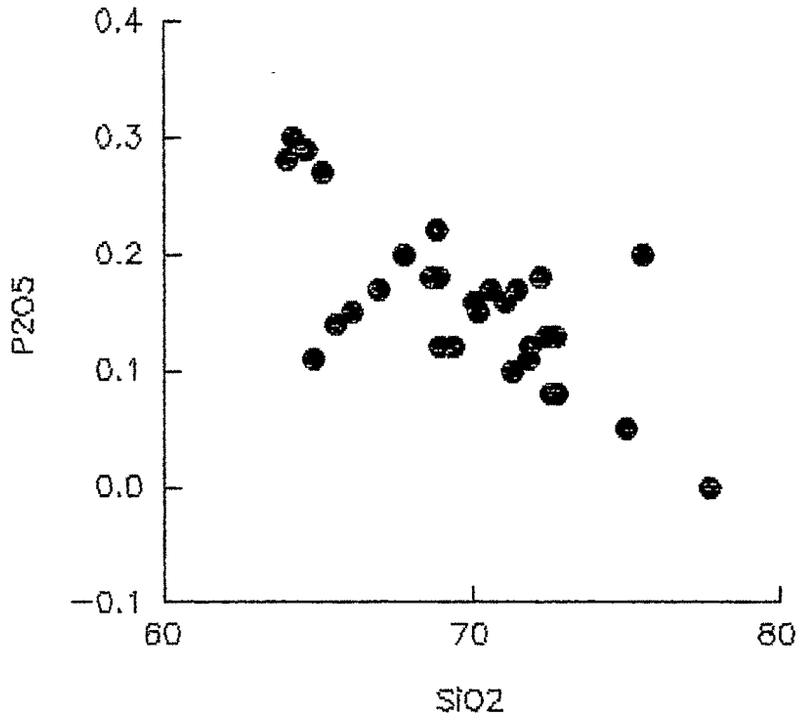

Fig. VI.7 c : P2O5 vs SiO2

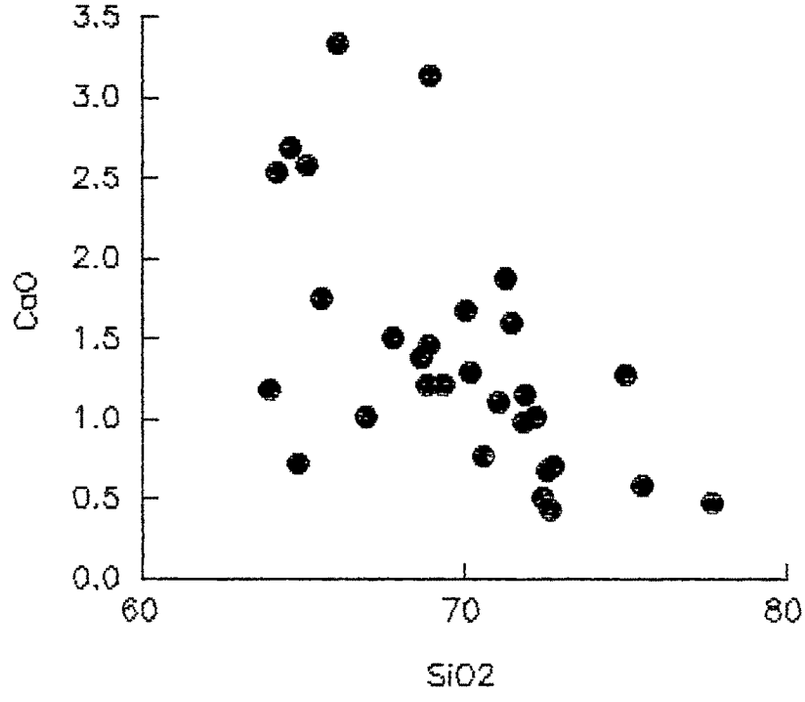

Fig. VI.7 d : CaO vs SiO2

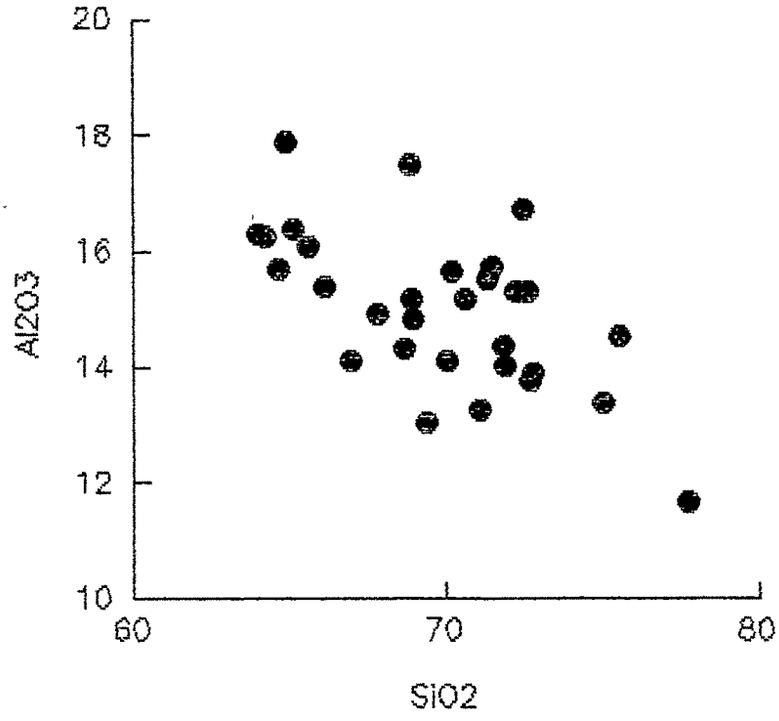

Fig. VI.7 e : Al2O3 vs SiO2

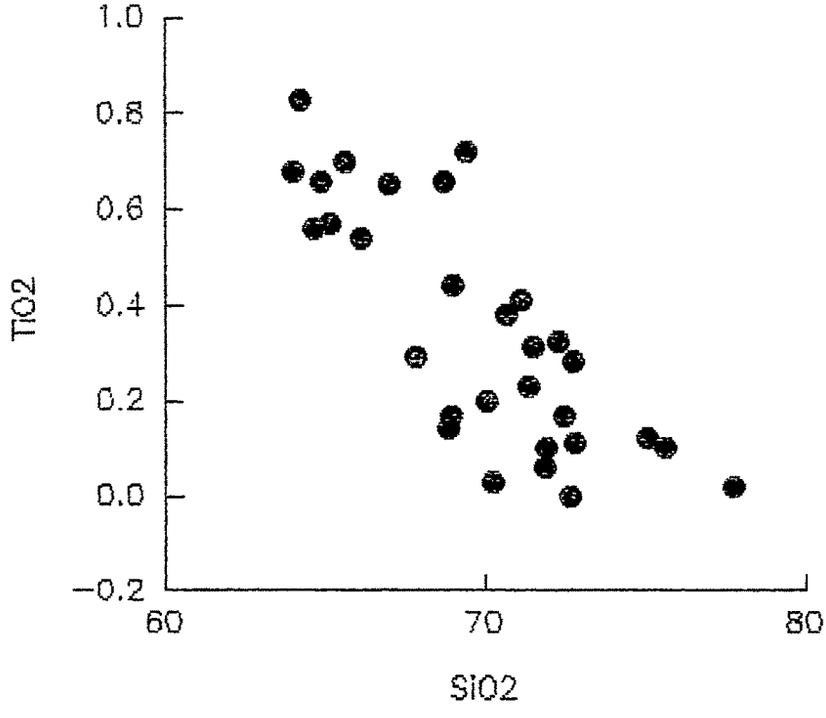

Fig. VI.7 f : TiO2 vs SiO2

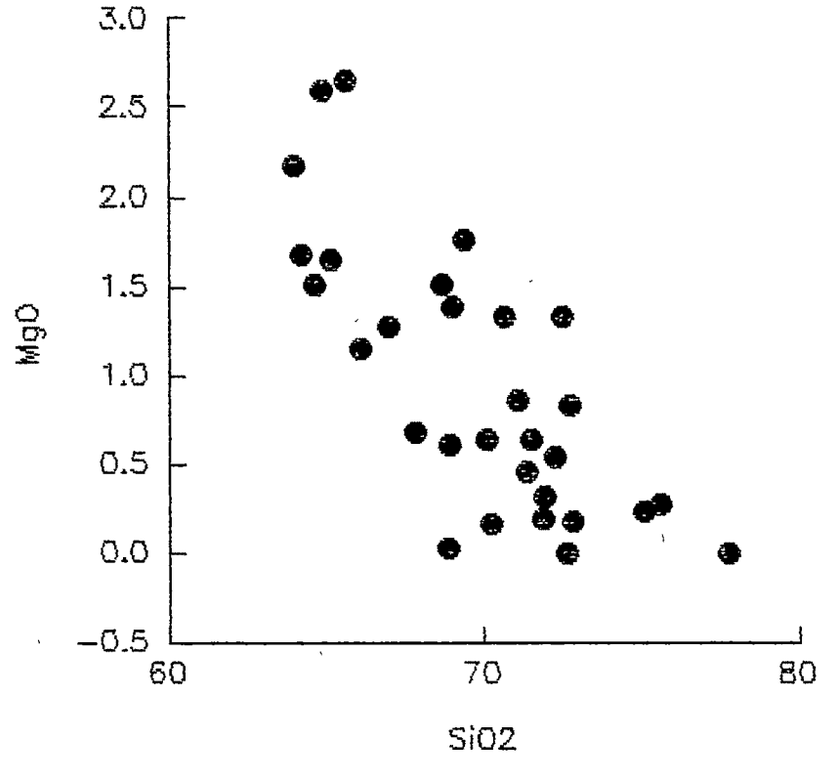

Fig. VI.7 g : MgO vs SiO2

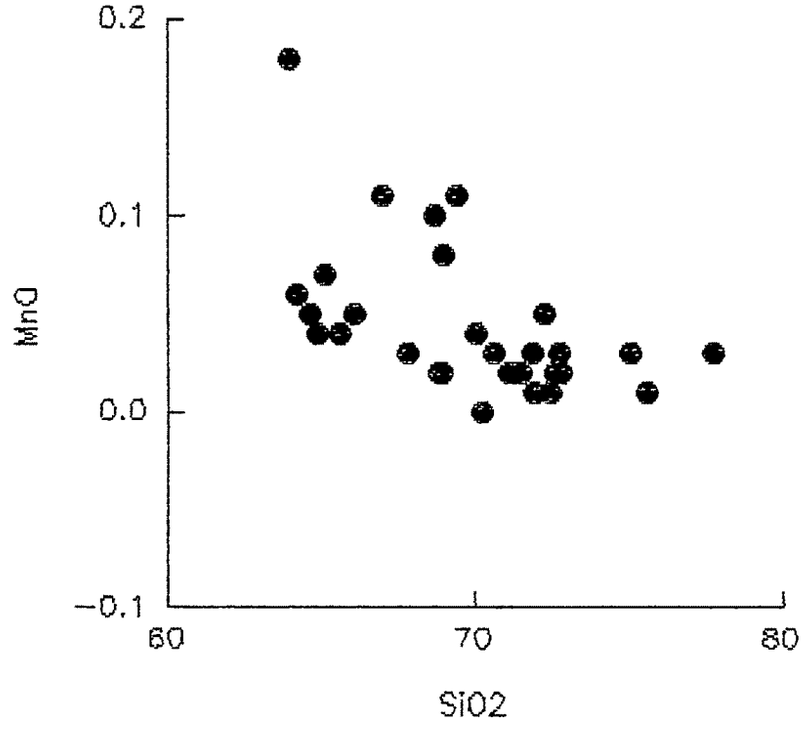

Fig. VI.7 h : MnO vs SiO2

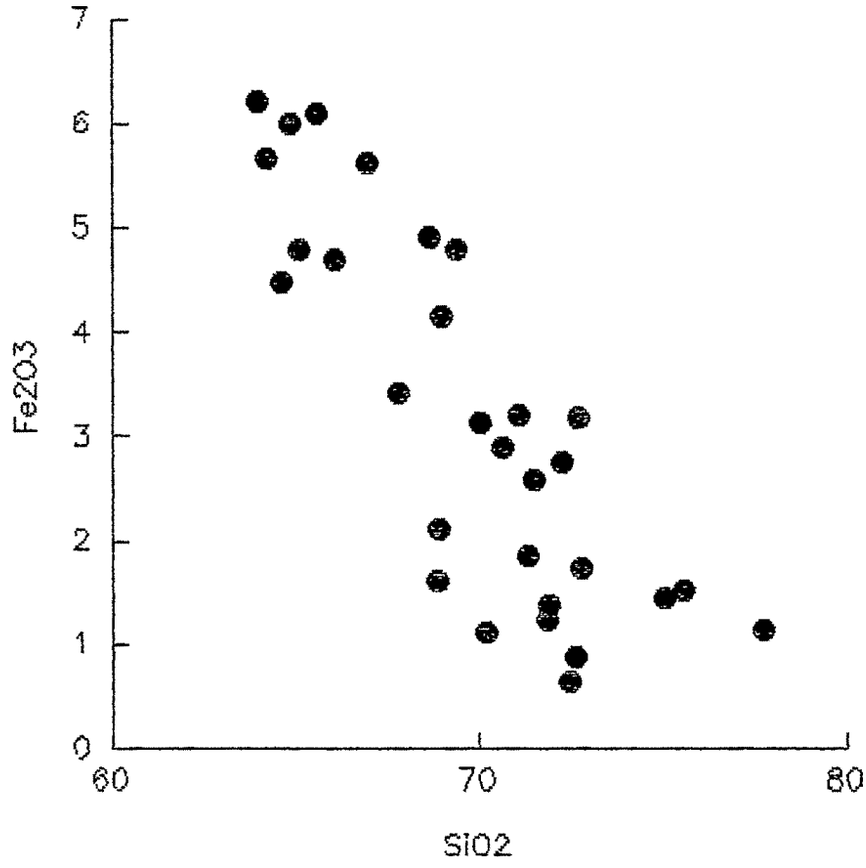

Fig. VI.7 i : Fe203 vs SiO2

Table VI.4 : Comparative average chemical analyses of various pelitic sediments and granitoid rocks of present study.

	Average sediment (Garrels and Mackenzie, 1971).	Average Archean Paragneiss. (Ronov and Migdisov, 1971)	Average Early Proterozoic Phyllites,Schists and Paragneisses. (Ronov and Migdisov, 1971)	Average of Granitoid rocks. Present study.	Average S-type Granites. Whalen et al., 1987)
SiO_2	59.7	64.15	58.42	70.46	70.27
TiO_2	–	0.48	0.79	0.19	0.48
Al_2O_3	14.7	15.79	16.63	14.95	14.10
Fe_2O_3(T)	6.1	5.98	6.56	2.74	2.87
MgO	2.6	2.45	4.12	0.74	1.42
CaO	4.8	4.02	2.34	1.33	2.03
Na_2O	0.9	2.84	1.57	3.62	2.41
K_2O	3.2	2.32	3.08	4.57	3.96
P_2O_5	–	0.14	0.09	0.14	0.15
MnO	–	0.07	0.15	0.04	0.06
	91.9	98.24	93.75	98.74	97.75

and TiO_2 when compared to the average sediment composition. However, it shows a close similarity to the average composition of S-type granite of Whalen et al. (1987).

On AFM diagram of Kuno (1968) the rocks of the study area indicate a calc-alkaline trend (Fig. VI.8). From this diagram it is also evident that there is a progressive enrichment in alkalies and concomittant depletion in magnesia and total iron. The calc-alkaline character of these rocks is also substantiated by the plots of $\log(CaO/Na_2O+K_2O)$ versus SiO_2 (Fig. VI.9), which is known as alkaline-lime index of Brown (1982). In this diagram all the points representing granitoids fall in the alkali-calcic field. Such evidence corroborates the conclusions of petrographic and field features.

Chappel and White (1974) used a variety of criteria to distinguish granitoid rocks. Probably, the most straight forward characteristic of S-type granites is their peraluminous composition, because pelites are relatively enriched in Al during weathering and so presumably will be metamorphic rocks derived from them. Hence, peraluminous nature is the most obvious S-type characteristic. The alumina saturation index of the granitoid rocks of the study area is more than 1, indicating their peraluminous nature. Even Niggli al>alk+C confirm their peraluminous nature. Molecular proportions of $Al_2O_3/CaO+Na_2O+K_2O$ versus SiO_2 were used by Chappel and White (1974) to indicate nature

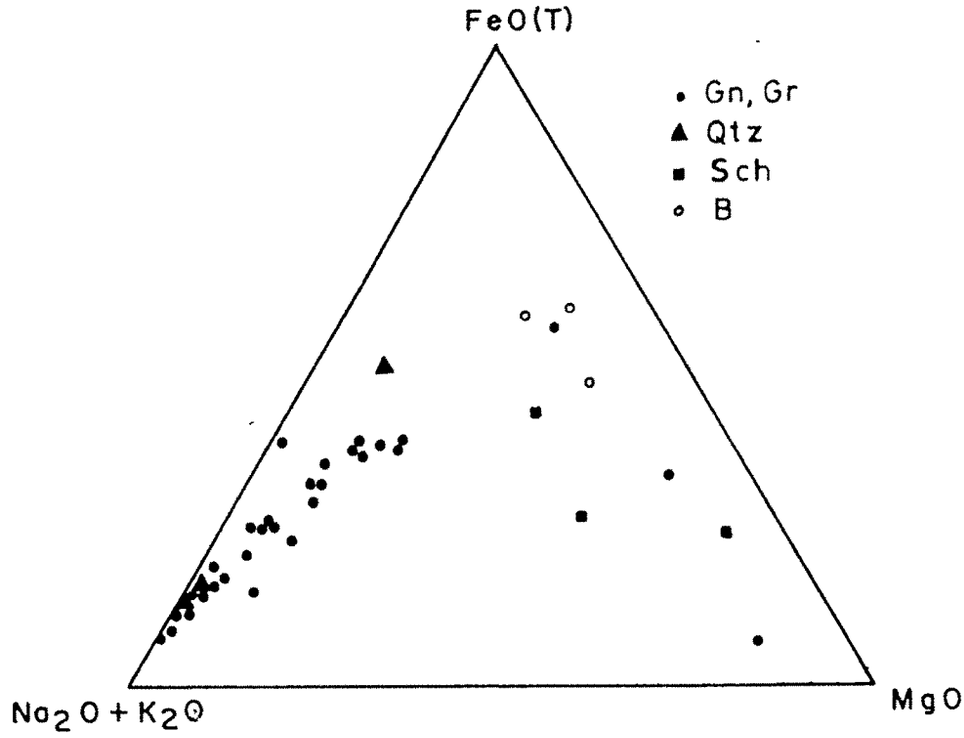

Fig.vi 8 AFM diagram (Kuno, 1968)

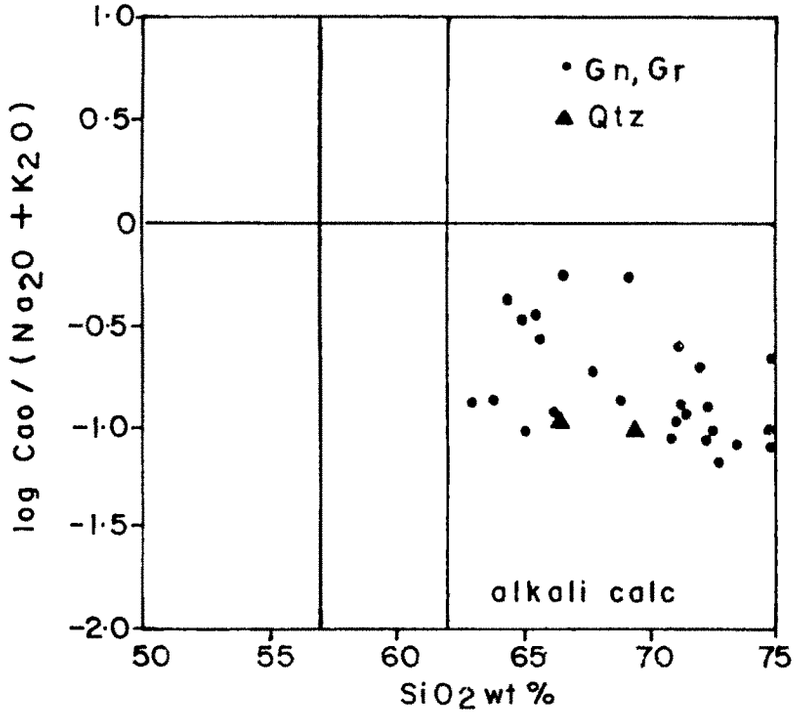

Fig.vi.9 Alkali lime index diagram
(Brown, 1982)

of source material. Almost all granitoid rocks of the study area plot in the S-type field (Fig. VI.10). Moreover, Garrel and Mackenzie (1971) used Na_2O/Al_2O_3 versus K_2O/Al_2O_3 diagram to delineate the sedimentary and igneous fields. Almost all rock samples of the study area including schists, quartzites and granitoids plot in the sedimentary field (Fig. VI.11). Only the amphibolites show a clear cut igneous origin exhibiting their ortho nature.

White and Chappel (1977) have also shown that K_2O versus Na_2O diagram is very efficient in demarcating between the fields of I- and S-granites of Barridale, Australia. Theoretically, alkalies are important parameters for discriminating between I-and S-granites. Relatively low Na_2O in S-type granites is due to removal of Na in sea water during sedimentary fractionation of source rock and high K due to its adsorption from the sea water into the clay minerals. When granitoid rocks of the study area were plotted in the K_2O versus Na_2O diagram (Fig. VI.12) most of the plots fall in the S-type field with two falling in the I-type field which could probably be due to a certain amount of overlap in both these fields.

TiO_2 which is highly correlated with Zr, and therefore decreases regularly with differentiation, P is tied up principally in small quantities of apatite and monazite, minerals that also appear to decrease modally with differentiation. However, in P_2O_5 versus TiO_2 diagram (Fig. VI.13), P_2O_5 shows no correlation

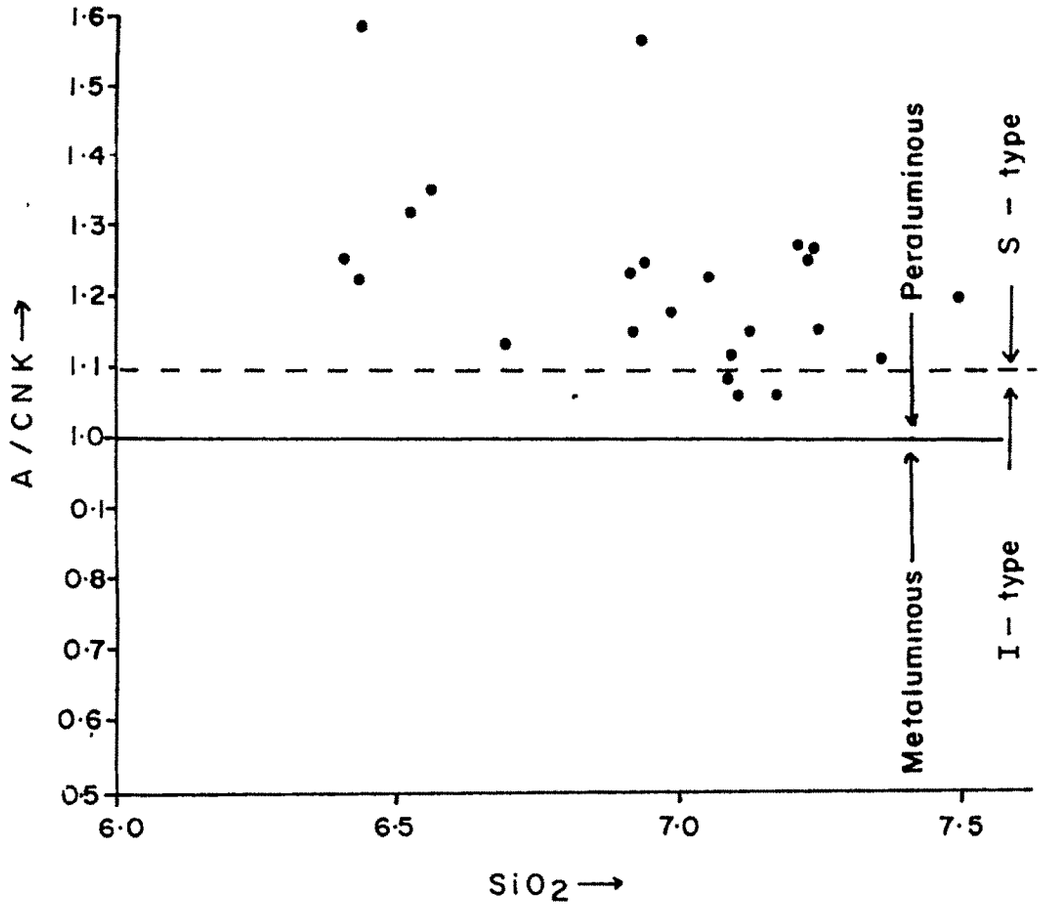

Fig. vi. 10 Chemical composition and presumed origin (I - S scheme of Chappell and White, 1974)

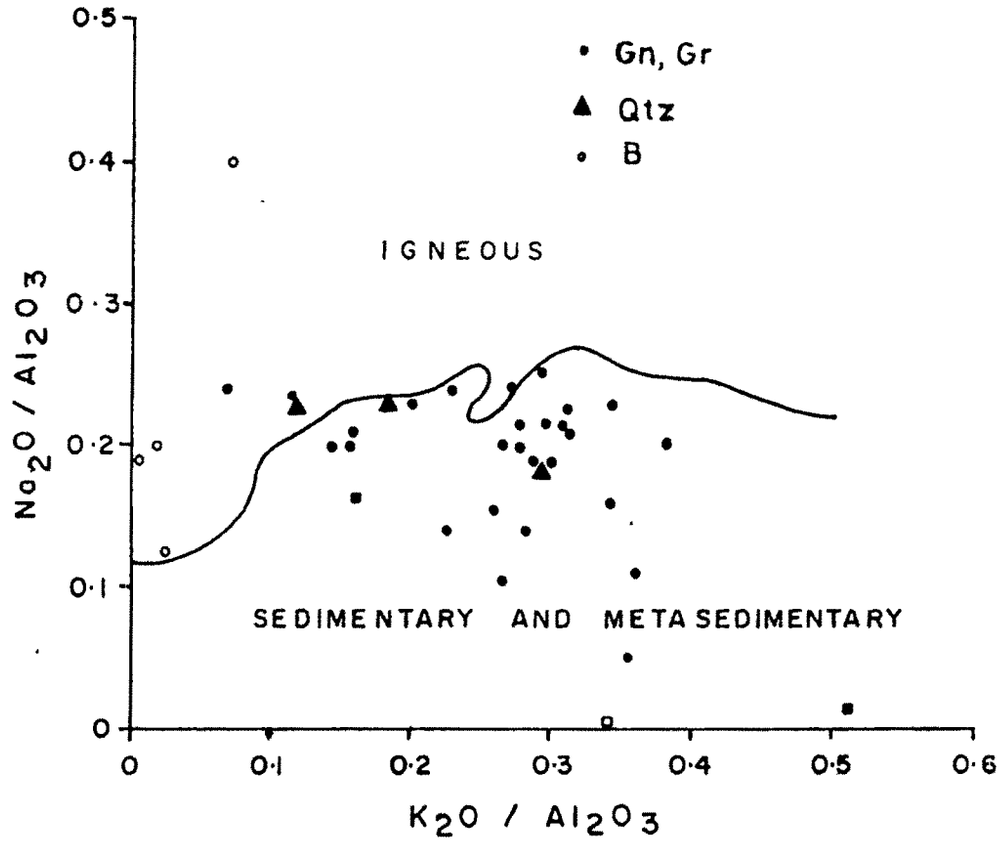

Fig. vi. II Na_2O / Al_2O_3 vs K_2O / Al_2O_3 Variation diagram. Fields of igneous and metasedimentary rocks (Garrel and Mackenzie 1971)

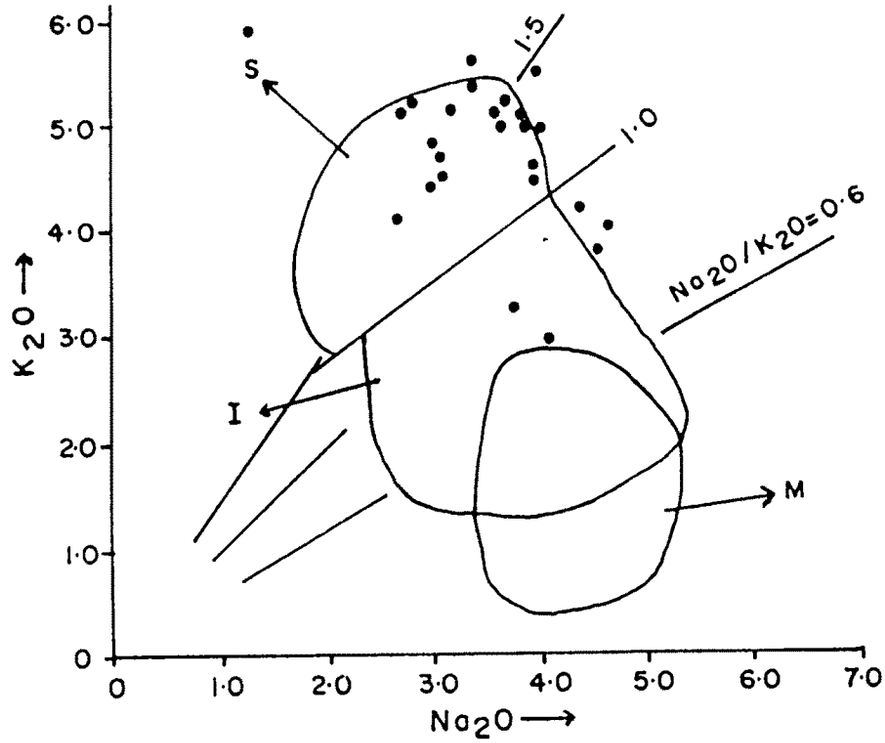

Fig. vi.12 K_2O vs Na_2O plots showing fields of M-, S- and I-granites (White and Chappell, 1977)

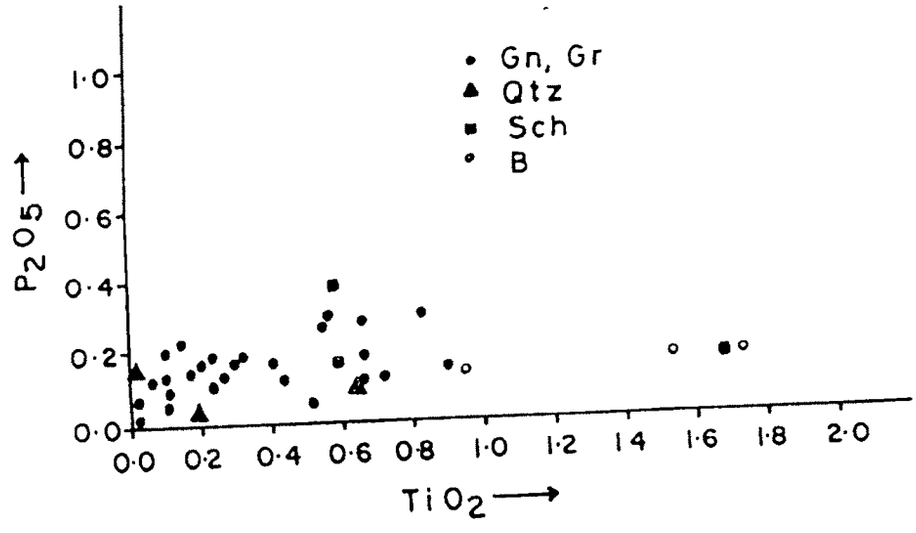

Fig. vi.13 P_2O_5 vs TiO_2

whatsoever with differentiation, indicating that its concentration are not related to an igneous melt fractionation processes.

The complementary diagram of de la Roche (1978) was chosen to plot the data aimed at establishing the connection between the chemical and the mineralogical compositions. This diagram clearly distinguishes parent sedimentary domains and can also estimate the relative proportions of quartz, feldspar and sheet silicates. Hence, in the Al/3-K versus Al/3-Na diagram major petrographic compositions occupy a distinct field in the diagram of quartzites, sandstones, arkoses, graywackes and shales. The granitoid rocks of the study area plot in the arkose field (Fig. VI.14).

Tectonic setting, however, provides a critical constraint on any modern granitoid classification. A simple but important division can thus be implied between continental granitoids generated during the evolution of fold belts (orogenic) and those granitoids more closely associated (anorogenic) (Bowden et al., 1984). Molar $Al_2O_3/(Na_2O + K_2O)$ versus molar $Al_2O_3/(CaO + Na_2O + K_2O)$ characteristics based on Shand's index were used by Maniar and Piccoli (1989) to delineate various tectonic settings. The granitoid samples of the study area all fall in the continental collision granite zone and are also highly peraluminous (Fig. VI.15).

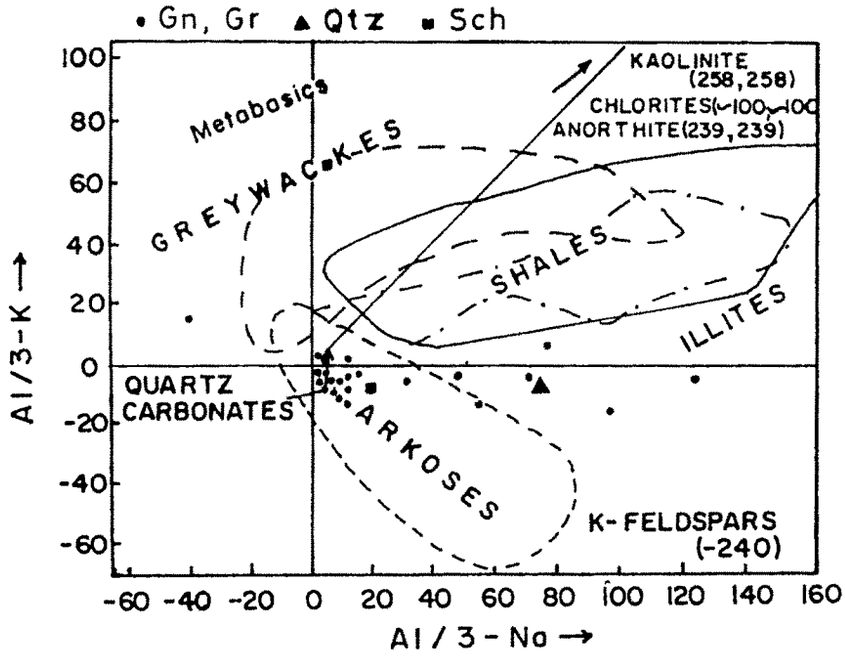

Fig. vi 14 Al/3-K vs Al/3-Na diagram for reference groups (de La Roche, 1978)

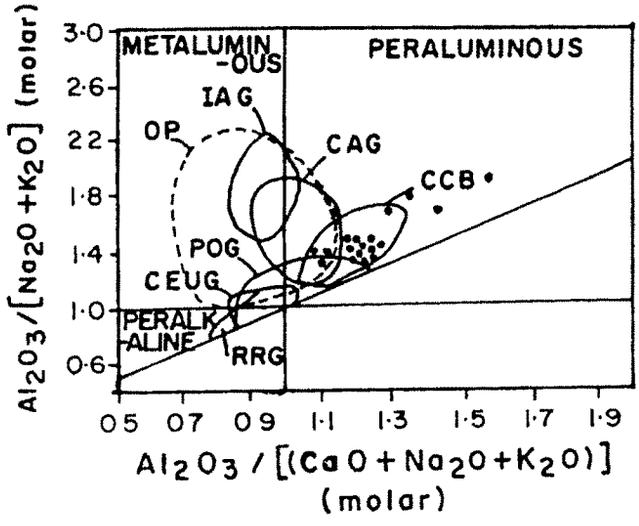

Fig. vi. 15 Shands index and various tectonic environments.
(Maniar and Piccoli, 1989)

TRACE ELEMENT CHEMISTRY

Trace element concentrations are generally used to study the nature of source rock or origin of a rock type and moreover trace elements when used in conjunction with other types of data often provide unique solution to petrologic problems. According to Shaw (1954) who investigated minor and trace elements of a series of pelitic rocks that had undergone progressive regional metamorphism, revealed that the concentration of most elements remained constant during metamorphism.

The rocks of Higher Kumaun Himalaya as well as of the various Lesser Himalayan nappes are supposed to have undergone progressive regional metamorphism during Precambrian and the most granitoids have formed during this metamorphism under upper amphibolite facies. Assuming that their trace element concentrations would be retained, the author has preferred to dwell upon the trace element behaviour of the granitoids to understand their original nature. The author therefore selected 18 representative samples of the granitoids from Higher Kumaun Himalaya and 6 from the nappes for trace elemental chemistry. The data on important trace elements are presented in Table VI.5.

A careful examination of the trace element data reveals that the Ni, Cu, Co, and V, show low concentrations ranging from 1.44 to

Table VI.5 TRACE ELEMENT ANALYSES OF ROCK SAMPLES

SL.NO.	SAMPLE NAME	ROCK TYPE	LOC.	Ni	Cu	Zn	Ga	Pb	Th	Rb	Sr	Y	Zr	Nb	Cr	Cs	U	Co	Ba	V
3	BJ1	Gn	BAJ	14.36	10.11	23.82	22.28	43.34	16.85	275.19	100.66	43.88	10.75	8.49	19.80	10.26	2.47	5.07	345.79	27.06
7	C3	Gn	CHP	9.94	6.22	49.95	20.80	19.96	20.44	212.88	93.97	36.65	0.44	11.63	24.82	5.29	3.13	2.97	675.31	37.07
10	D3	Gn	ASK	7.13	5.01	24.68	24.67	30.16	17.10	589.80	11.66	22.51	0.78	17.11	5.46	26.07	5.74	2.35	15.47	4.28
12	L24	Gn	CCY	6.16	17.77	77.64	19.73	49.06	55.73	401.32	89.91	60.39	200.12	14.01	-	-	-	-	-	-
13	M1	Gn	CCY	8.89	26.79	62.76	22.18	50.43	23.16	111.43	284.94	31.09	494.84	20.82	-	-	-	-	-	-
14	M10	Gn	CCY	8.94	25.04	40.42	16.82	35.03	30.77	101.97	97.03	32.55	338.19	12.55	-	-	-	-	-	-
15	M11	Gn	CCY	10.69	43.89	56.04	18.16	58.44	57.18	136.84	63.02	56.72	418.33	19.77	-	-	-	-	-	-
19	M15	Gn	CCY	9.75	26.43	69.81	15.62	45.02	33.45	137.13	86.83	38.08	486.66	12.75	-	-	-	-	-	-
25	M2	Gn	CCY	8.77	25.47	67.60	19.97	50.02	28.84	142.68	321.46	23.95	211.63	13.28	-	-	-	-	-	-
26	M20	Gn	CCY	4.67	11.25	52.47	18.75	41.09	81.03	260.21	56.12	56.30	255.36	19.84	-	-	-	-	-	-
31	M4	Gn	CCY	9.88	27.57	90.49	21.88	52.98	53.56	207.10	233.02	42.02	375.79	16.49	-	-	-	-	-	-
33	M5	Gn	CCY	6.00	16.13	57.98	21.72	43.75	79.03	372.43	93.06	52.16	243.78	11.18	-	-	-	-	-	-
35	M7	Gn	CCY	4.09	9.64	45.77	18.36	48.06	57.22	357.68	85.97	41.04	153.35	4.73	-	-	-	-	-	-
36	M8	Gn	CCY	14.71	39.72	66.36	18.02	42.73	54.78	133.05	182.37	31.03	496.31	19.14	-	-	-	-	-	-
38	N21	Gn	CCY	1.44	2.14	29.60	16.55	34.47	34.44	116.71	80.39	24.90	137.49	6.20	-	-	-	-	-	-
39	N23	Gn	CCY	1.16	2.67	41.36	19.77	54.15	27.97	381.18	90.85	42.55	94.93	7.53	-	-	-	-	-	-
16	M12	Gr	CCY	2.49	3.48	29.85	12.79	25.07	15.52	76.51	95.21	26.74	132.22	5.89	-	-	-	-	-	-
18	M14	Gr	CCY	3.94	12.50	67.10	17.76	82.53	44.53	271.37	136.65	67.06	148.89	14.86	-	-	-	-	-	-
21	M17	Gr	CCY	25.12	44.97	37.61	19.61	63.40	1.18	387.92	49.77	10.99	0.23	1.67	180.48	22.13	22.79	0.04	108.88	137.82
2	A2	Gr	ALM	7.81	8.78	61.49	22.81	28.67	18.60	350.76	64.68	13.10	1.33	16.90	14.85	21.67	1.15	2.93	384.33	-
17	M13	Gr	CCY	3.20	7.15	49.18	18.70	70.75	43.67	328.91	74.69	52.66	115.46	8.15	-	-	-	-	-	-
20	M16	Gr	CCY	3.53	9.00	54.55	17.54	52.05	18.60	311.00	121.55	33.66	64.45	5.10	-	-	-	-	-	-
9	C7	Gr	CAM	33.80	10.83	57.76	31.03	106.37	7.71	183.52	188.31	178.21	176.32	10.97	60.70	6.98	1.18	14.62	544.34	100.93
1	A1	Gr	ALM	3.26	9.08	69.22	19.72	42.24	51.34	265.21	111.03	41.30	135.89	12.48	-	-	-	-	-	-

25.12 ppm (Ni), 2.14 to 44.97 ppm (Cu), 0.04 to 14.62 ppm (Co) and 19.43 to 184.91 ppm (V), like those of crustal granites.

The concentration of Rb in the granitoids of the study area is 101.9 to 589.8 ppm; which is rather high and typically represents its derivation from pelitic rocks. It appears that it survived a sustained weathering, and there has been no change in its concentration during metamorphism. Sr concentration which varies from 11.66 to 321.46 ppm is rather low. The high and low concentration of Rb and Sr in the granitoid rocks indicate that these could have formed due to the granitisation of pelitic rocks. This is in accordance with what Miller (1984) has mentioned that Rb and Sr concentrations tends to be rather high and rather low respectively in the pelites. Further these rocks exhibit Rb/Sr ratio of the order of 0.8 to 7.79 which is considerably high and again point to their pelitic nature. According to Miller (1984) the Rb/Sr ratios of pelites and their metamorphosed equivalents are much higher than those of average crustal rocks (0.5 - 1).

Only 6 samples of granitoids could be analysed for Ba concentrations (Table VI.5) and it was found to range from 15.5 to 675.3 ppm, and in all cases was < 1000 ppm which is a characteristic of Ba content in pelitic rocks.

The average Rb/Ba ratio for the granitoid rocks is as high as 7.3 and this ratio also distinctively points towards a pelitic

source. In the pelites Rb/Ba ratio is generally higher than the crustal average ratios (of the order of 0.25) and these ratios would be even higher in co-existing liquids because partition coefficients are higher for Ba for all relevant crystalline phases than for Rb (Miller, 1984). Ga which remains more or less constant, ranges from 12.79 to 31.03 ppm.

Harker diagrams have been used to understand the behaviour of certain trace elements with respect to SiO_2. While Zr and Zn are found to decrease with increasing silica, Y and Ga remain more or less unchanged with increase in silica (Figs.VI.16 a, b, c and d). In the Rb vs MgO (Fig.VI.17), it is observed that there is an increase of Rb with decreasing MgO. This could very well be attributed to action of fluid phases (Clarke, 1992). It is known that Sr is strongly partitioned into plagioclase, and the CaO vs Sr diagram (Fig.VI.18) shows that with increasing CaO, Sr is also increasing exhibiting positive correlation. Both Rb and Sr, hence confirm their compatible nature.

Co-variation of two elements, usually with similar geochemical behaviour and competing for the same lattice sites helps to define the processes of chemical evolution. In Fig.VI.19 both the large ion lithophile elements Rb vs K are compared and they reveal a positive correlation and low K/Rb ratios. Conventional wisdom suggests that high K/Rb ratios are typical of magmatic processes and that lower values can only be reached by fluid interaction.

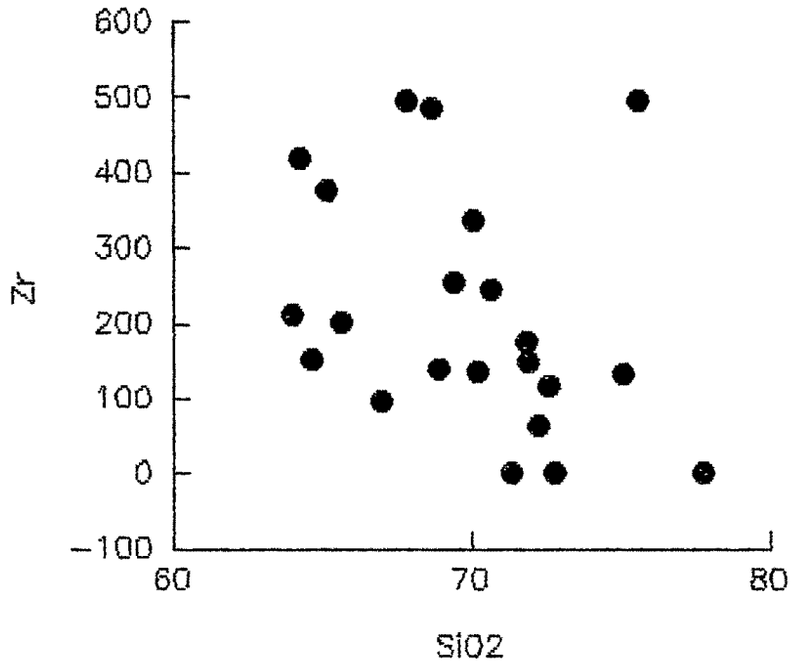

Fig. VI.16a : Zr vs SiO2

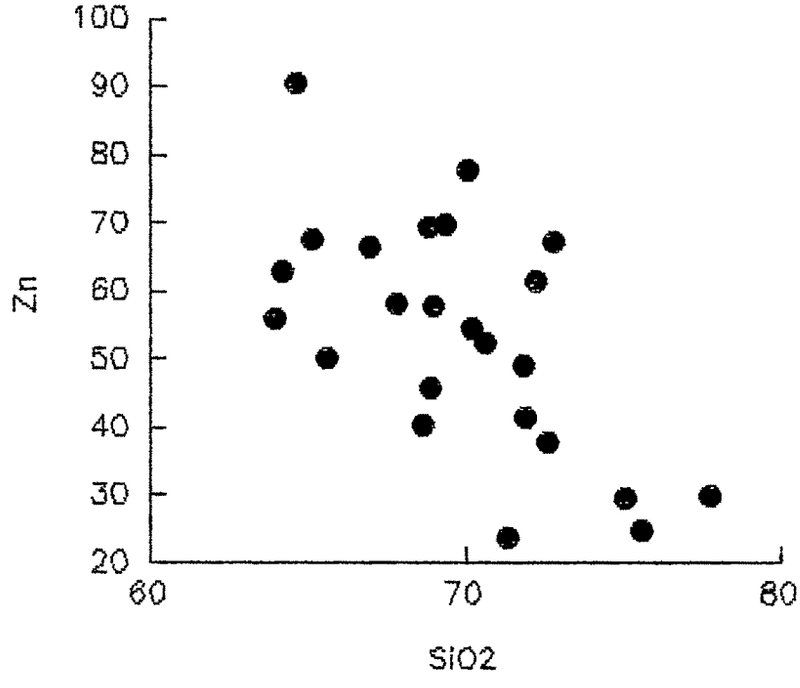

Fig VI.16b : Zn vs SiO2

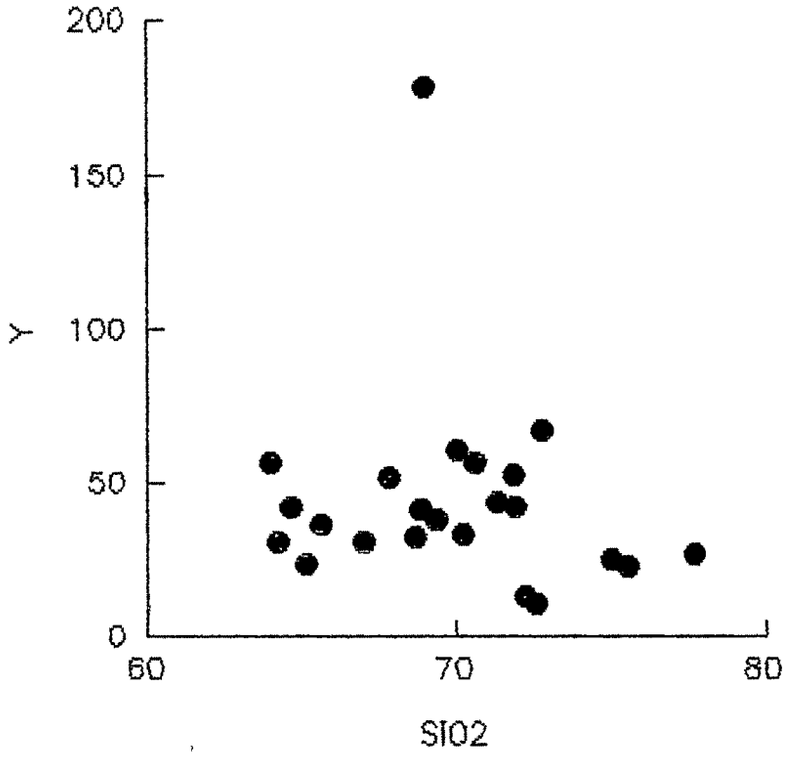

Fig. VI.16c : Y vs SiO2

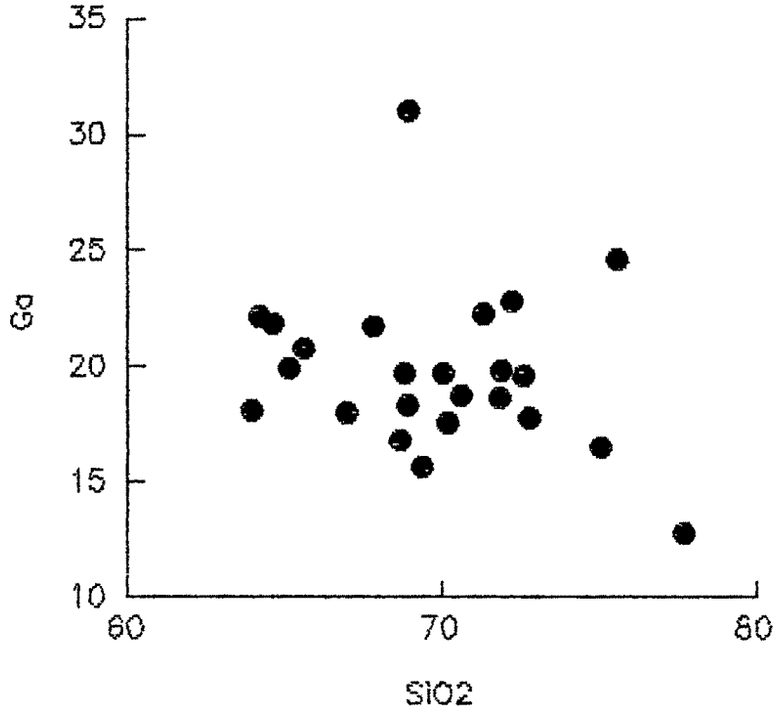

Fig. VI.16 d : Ga vs SiO2

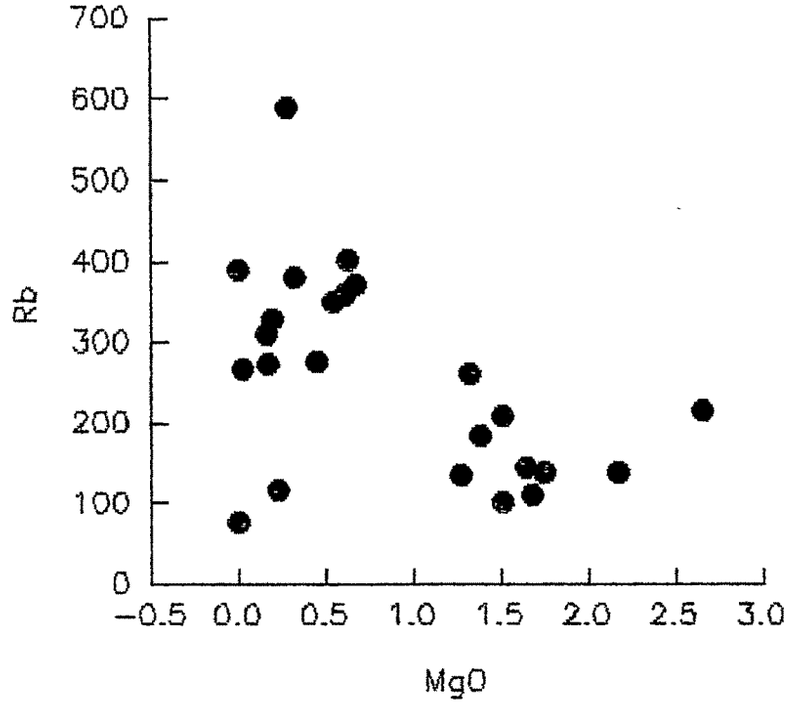

Fig. V!.17 : Rb vs MgO

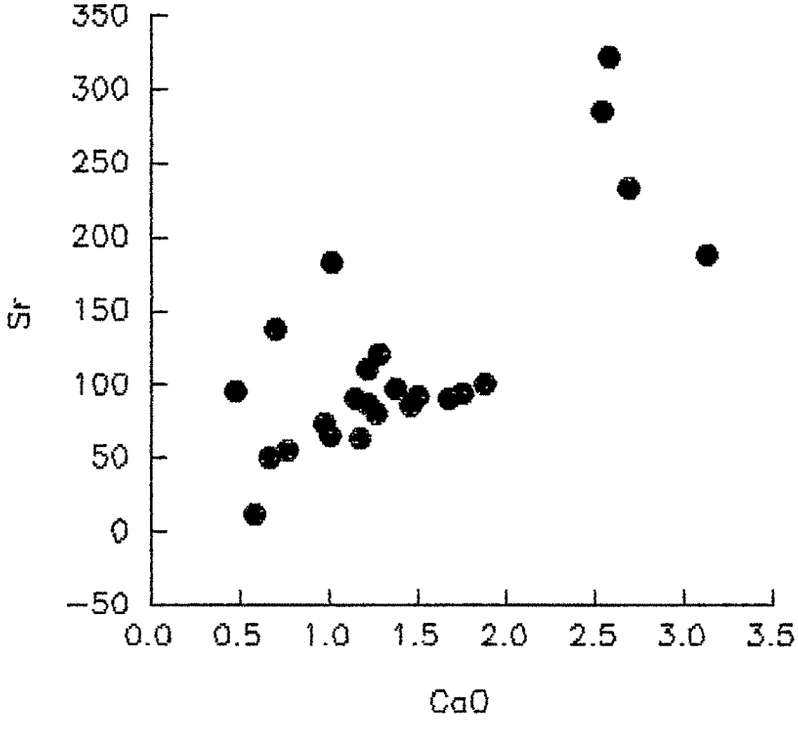

Fig. VI.18 : Sr vs CaO

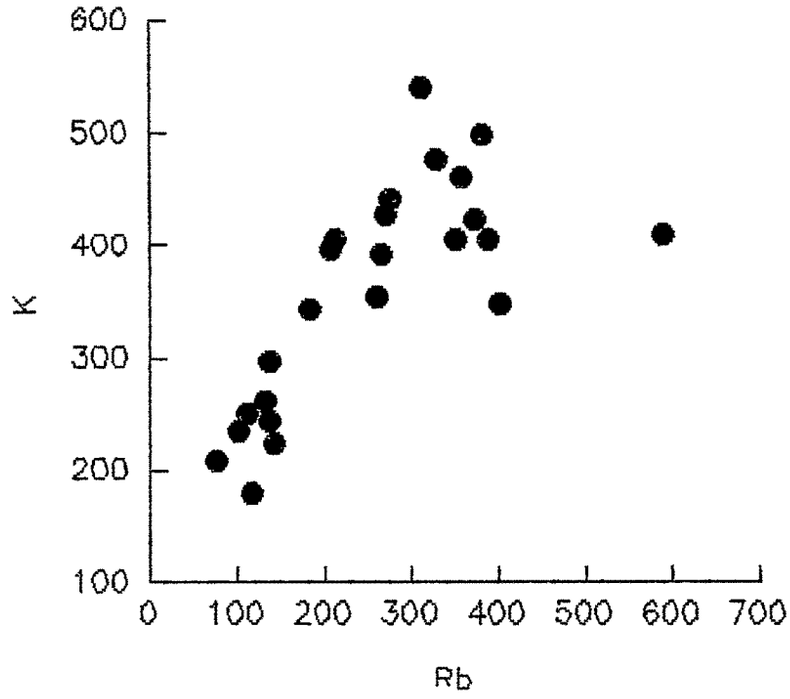

Fig. VI.19 : K vs Rb

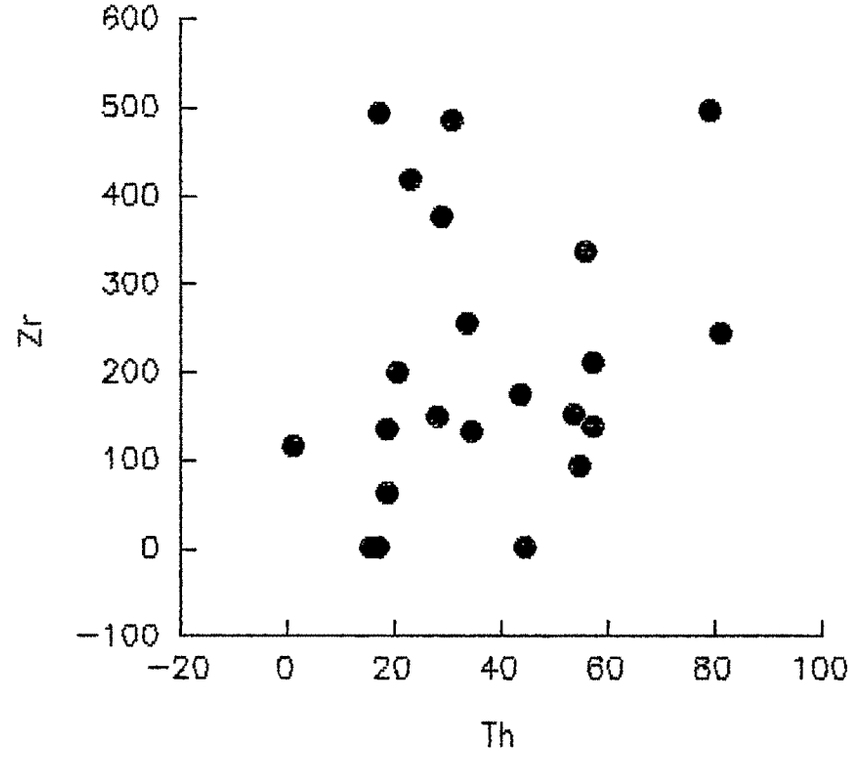

Fig. VI.20 : Zr vs Th

While the high field strength elements Th and Zr when plotted (Fig.VI.20), reveal that there is almost no change in Th with little change in Zr, indicating removal of Zircon has not been a part of the process of formation of these rocks. The Zr concentration has as expected,thus remained more or less unchanged during the evolution of these rocks.

Using Rb-Sr systematics the granitoids can be primarily grouped into two genetic end members those derived from the mantle (M - and I - granite) and those from the continental crust (S - and A - granites). Using Misra and Sarkar's (1991) diagram (Fig. VI.21) it is observed that almost all the granitoids of the study area fall in S - granite field. A few plots fall in the A - type field also and this discrepancy could be attributed to a certain degree of overlap between S - and A - type granite fields, indicating their sources in continental crust or derived material from it.

Trace element discrimination diagrams for interpreting the tectonic setting of the granitoids have received less attention than those for basalts perhaps due to the problem of sampling granitoids with well defined tectonic settings and their complicated petrogenetic histories which make their chemical compositions difficult to interpret. Pearce et al. (1984) classified granitoids of known tectonic setting on the basis of their geochemical and mineralogical characteristics, using K, Rb,

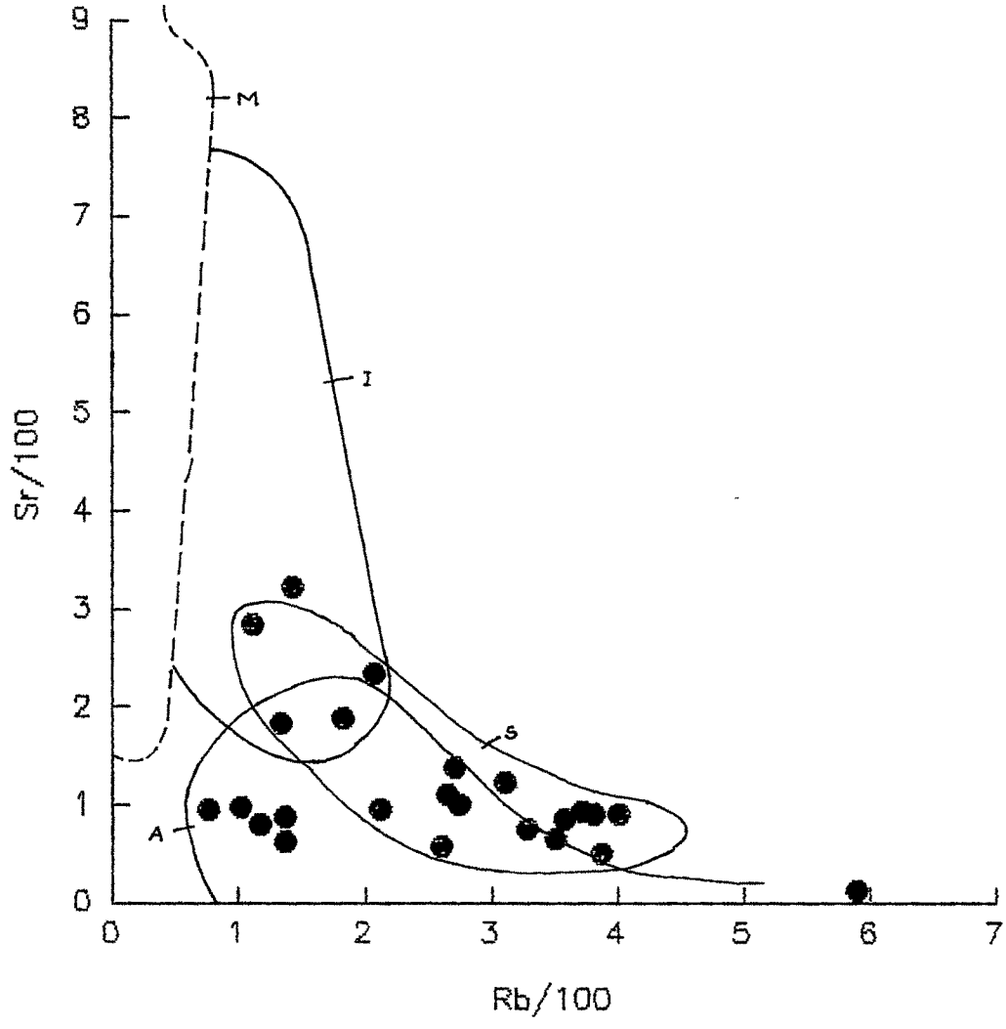

Fig. VI.21 : Sr/100 vs Rb/100

Sr, Y, Zr and Nb as the discriminants. They divided granitoids into Ocean Ridge Granites (ORG), Volcanic Arc Granites (VAG), Within Plate Granite (WPG), and Collision Granites (COLG) which were further subdivided into Syn-Collisional and Post-Collisional Granites. On Y vs SiO_2 and Nb vs SiO_2 discrimination diagrams (Figs.VI.22 and 23) the granitoids of Kumaun plot in the VAG, COLG and ORG fields, where as in the Nb vs Y diagram (Fig.VI.24) the granitoids get separated into VAG and syn-COLG fields. Further the Rb vs SiO_2 and Rb vs Y + Nb diagrams (Fig.VI.25 and 26) clearly discriminate the granitoids of the study area in the syn-COLG field. The Syn-Collision Granites thus as defined by Pearce et al. (1984) are typically muscovite bearing, peraluminous and exhibit most of the features associated with S-type granites.

RARE EARTH ELEMENT CHEMISTRY

The development of precise analytical techniques for the analysis of the individual rare earth elements (REE) have rendered them particularly valuable for placing limits on the applicability of proposed petrogenetic models. The REE are particularly useful in petrogenetic studies because they are geochemically very similar and have greatest abundance in minerals with sites preferring an element with a cation radius of about 0.9 to 1.0 angstrom. An important consideration in the application of REE to petrogenetic studies is the mobility of REE during metamorphism, hydrothermal alteration and weathering, as most of the rocks found at the

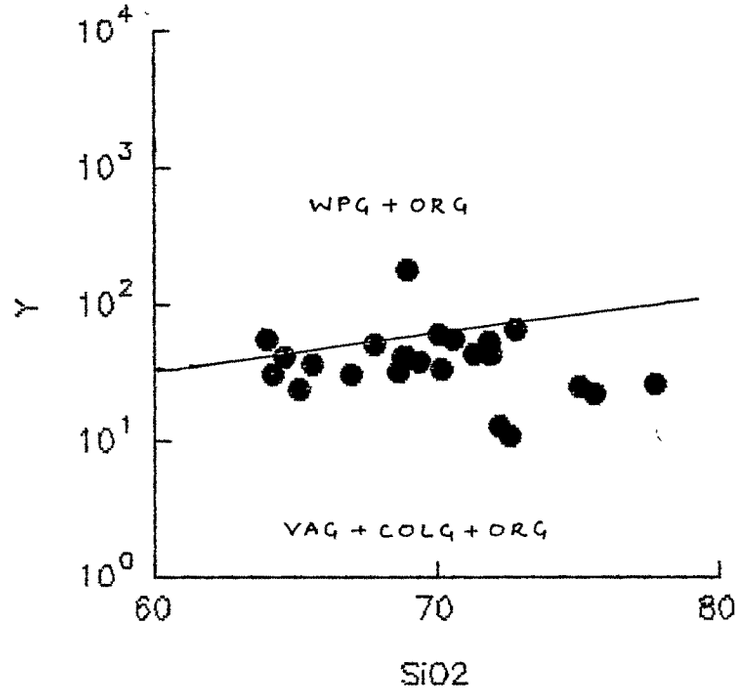

Fig. VI.22 : Y vs SiO2

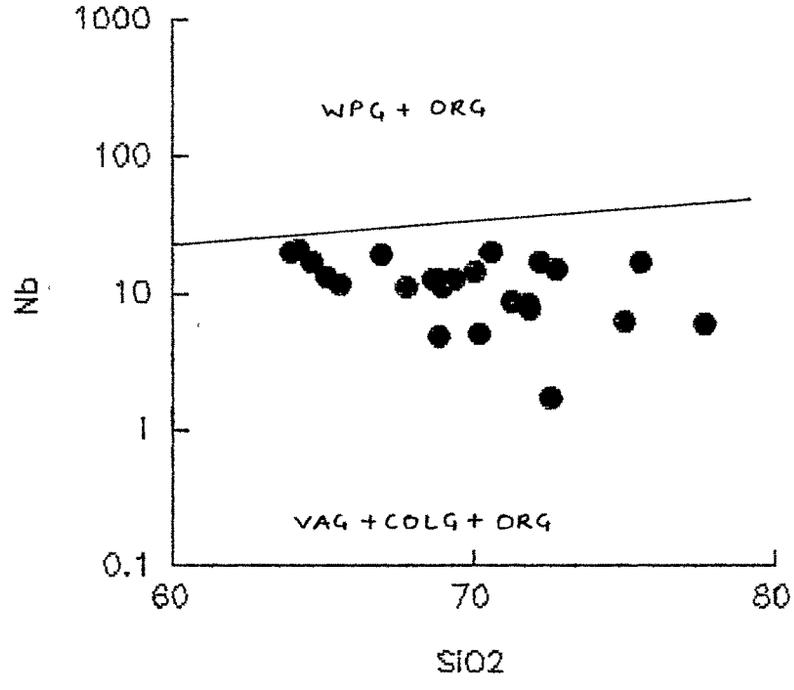

Fig. VI.23 : Nb vs SiO2

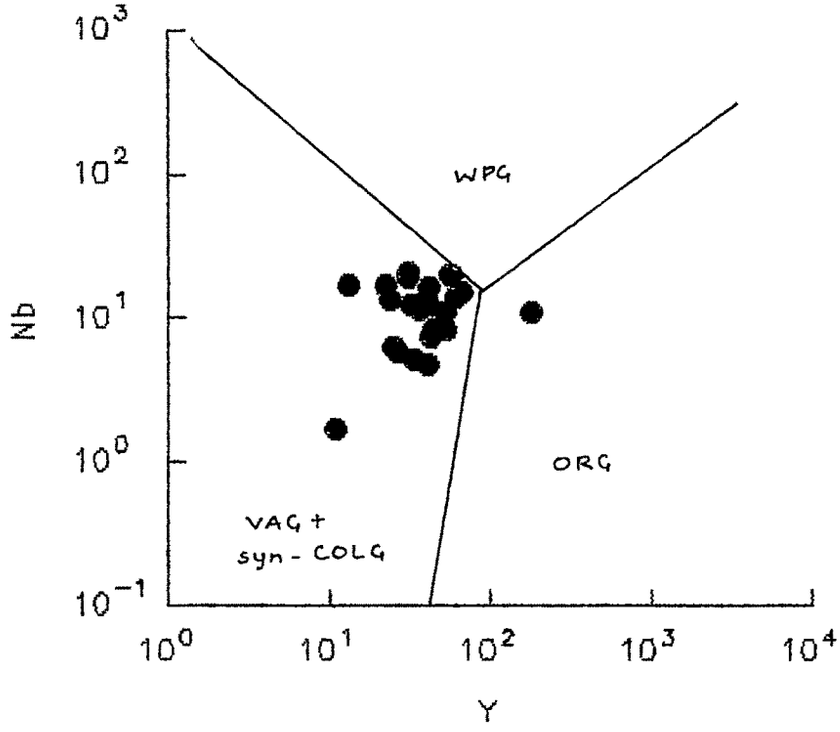

Fig. VI.24 : Nb vs Y

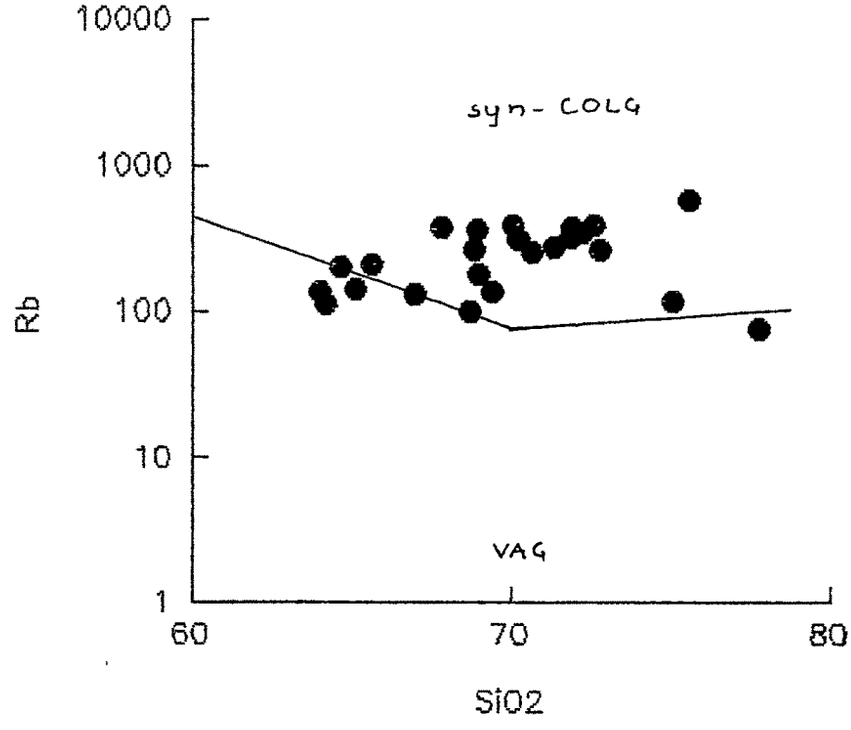

Fig. VI.25 : Rb vs SiO2

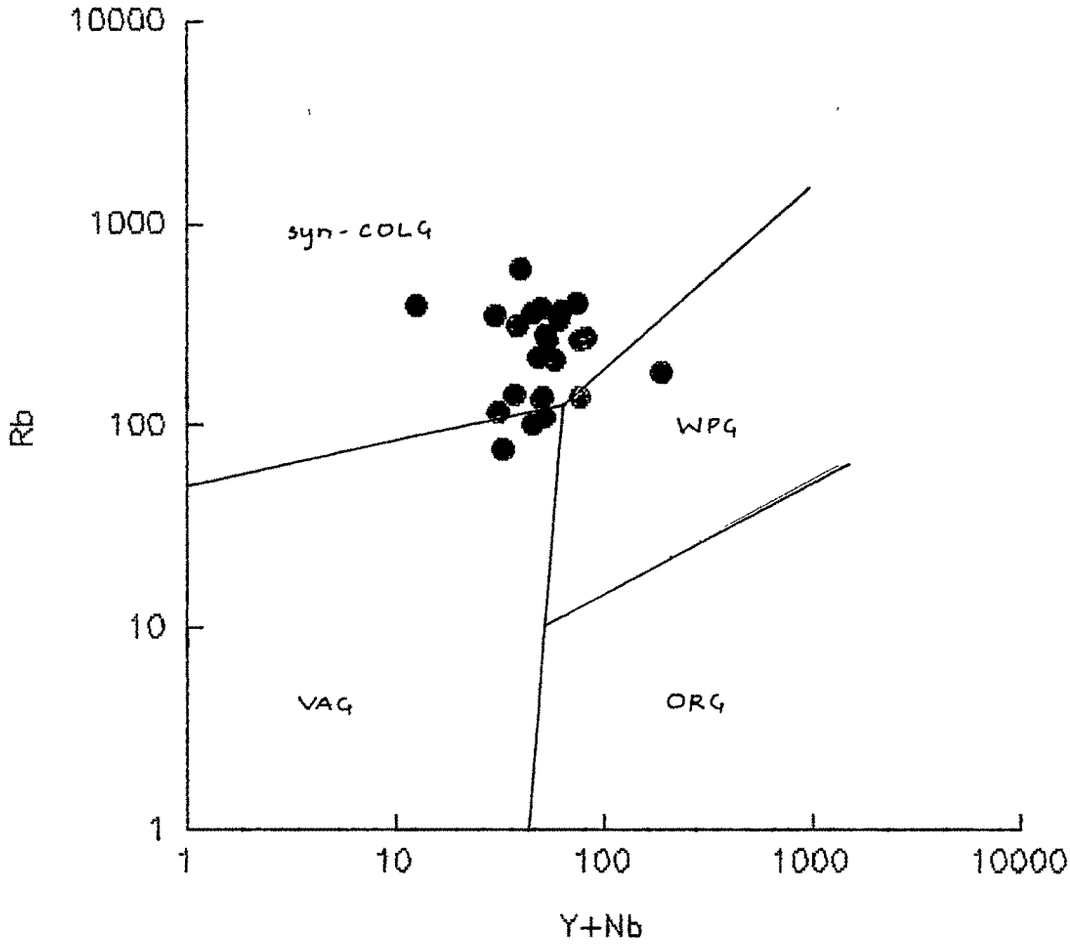

Fig. VI.26 : Rb vs Y+Nb

surface of the earth may have been affected by one or even all of these processes. However, unless these processes are obviously severe, they do not cause a major change in the patterns or abundances for the REE (Sun and Nesbitt, 1978). Hence, it appears that most rocks that have undergone essentially static metamorphism or only very limited hydrothermal alteration or weathering should give REE patterns and abundances indicative of the original rock. For REE analysis of any granitoid rock it is important to consider that the majority of these elements reside in trace mineral phases such as apatite, sphene, monazite, zircon, xenotime, etc (Bromet and Silver, 1978). Hence, a large rock sample enough to be representative has to be powdered and well homogenised to attain analytical precision. The REE data for the rocks of the study area are given in Table VI.6.

Spider diagrams enable comparison with any other composition, usually a general standard at a glance. Fig. VI.27 shows the average of granitoids of study area compared with average continental crust compositions (Clarke and Washington, 1924). While most of the LREE are found enriched, Er concentration remains unchanged and Y and Lu concentrations are found depleted. The deviation from the average continental crustal concentrations could be attributed to the mobility of the REE'S. The REE'S mobility under metasomatic conditions could be one of the main reasons as demonstrated by Corey and Chatterjee (1990).

Table VI.6 RARE EARTH ELEMENT ANALYSES OF ROCK SAMPLES

Sl No.	Sample	Rock Type	Loc.	La	Ce	Pr	Nd	Sm	Eu	Gd	Dy	Er	Yb	Lu
13	M1	Gn	CCY	97.19	154.65	7.92	64.65	14.91	2.97	7.98	10.65	4.29	4.29	0.41
36	M8	Gn	CCY	85.56	100.04	7.77	42.53	15.92	2.46	5.65	7.81	4.49	3.89	0.56
15	M11	Gn	CCY	141.42	180.21	35.41	81.36	83.32	10.30	16.05	11.97	5.87	5.35	1.15
3	BJ1	Gn	BAJ	96.86	81.62	10.26	25.81	16.61	1.43	96.86	3.00	1.37	0.66	0.09
10	D3	Gn	ASK	9.15	21.28	0.87	7.85	0.68	<0.01	1.67	4.01	1.18	1.28	0.06
7	C3	Gn	CHP	50.83	107.40	4.13	47.60	7.87	1.29	5.02	7.71	3.99	3.68	0.20
21	M17	Gr	CCY	5.94	9.46	0.37	2.76	0.38	0.15	0.61	1.49	0.51	0.52	<0.01
9	C7	Gr	CAM	160.36	314.96	14.89	57.14	28.89	4.20	6.88	10.31	3.36	2.16	0.16
2	A2	Gr	ALM	31.57	69.66	2.63	32.61	6.85	0.56	3.61	3.32	1.02	0.70	0.04
30	M3A	B	CCY	18.92	33.24	2.64	17.88	8.50	1.85	3.42	6.06	3.41	3.15	0.42

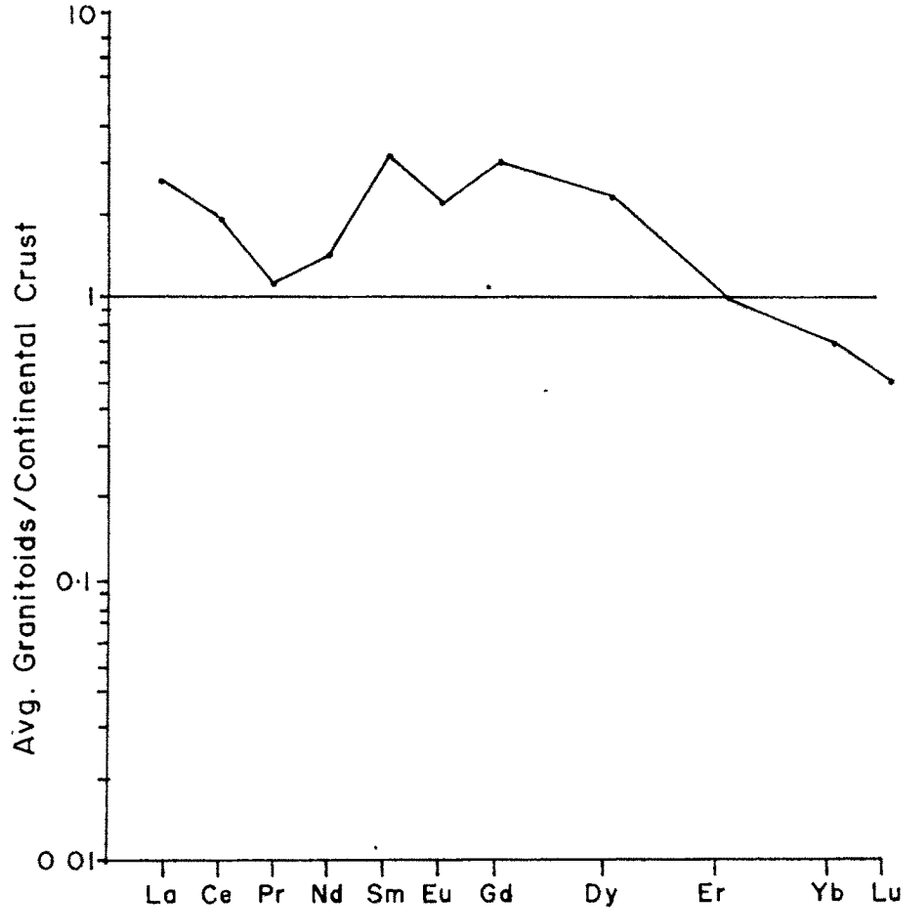

Fig. VI. 27 Spider diagram representing comparison of average REE abundances to that of average continental crust concentrations

The REE abundances for the granitoid rocks of the Central Crystallines as well as the crystalline nappes were normalised using chondrite normalising values given by Haskin et al. (1968) and plotted as shown in Fig. VI.28. These REE patterns more or less match with the calculated REE patterns of an original graywacke composition which was experimentally melted at amphibolite grade (Nance and Taylor, 1976). They showed that although there are some variations as a function of age, all analysed graywackes and shales have similar REE patterns and concentrations and they concluded that these concentrations were representative of the continental crust. Hence, since the REE patterns for graywackes approximates that of the continental crust, if large volumes of continental crust are involved in melting, the parent will probably have a REE composition similar to that of graywacke (Hanson, 1980). All LREE show almost identical slopes excepting sample number C7 which is showing slightly high Sm concentration, perhaps owing to some analytical error. The HREE are all give flat patterns while only two samples show slight depletion. Negative Eu anamolies betray removal of plagioclase. Similar REE patterns of all the granitoid samples suggest similar source and the similarity to the REE patterns of rocks derived from continental crust is in conformity with the major oxide and trace elemental data interpretation.

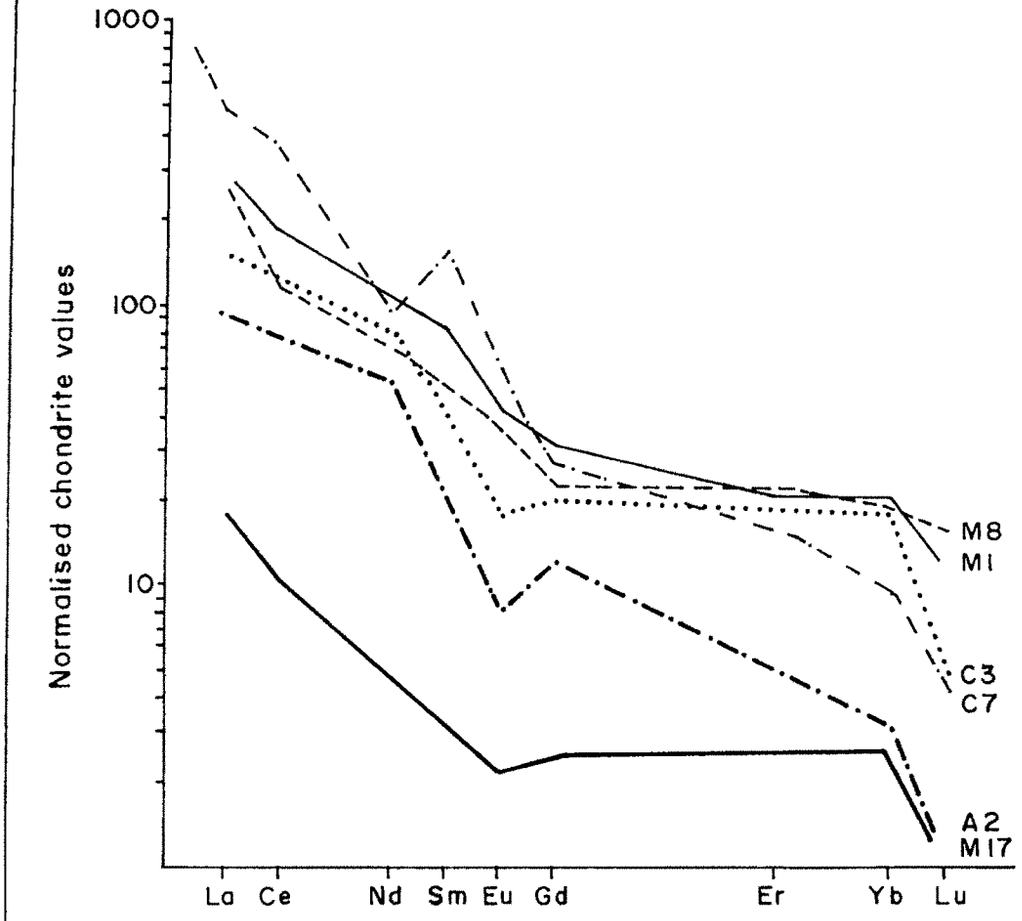

Fig. VI 28 REE patterns for granitoid rocks